Article Type: Full Paper

Hybrid Pharmacophore Design, Molecular Docking, Synthesis, and Biological Evaluation of Novel Aldimine-Type Schiff Base Derivatives as Tubulin Polymerization Inhibitor

Alieh Ameri,[a] Ghadamali Khodarahmi,[b,] Hamid Forootanfar,[c,**] Farshid Hassanzadeh,[b] Gholam-Hosein Hakimelahi,[b,d]*

[a] *Department of Medicinal Chemistry, Faculty of Pharmacy, Kerman University of Medical Sciences, Kerman, Iran*

[b] *Department of Medicinal Chemistry, Faculty of Pharmacy, Isfahan University of Medical Sciences, Isfahan, Iran, khodarahmi@pharm.mui.ac.ir (Gh. Khodarahmi)*

[c] *Department of Pharmaceutical Biotechnology, Faculty of Pharmacy, Kerman University of Medical Sciences, Kerman, Iran, forootanfar@yahoo.com*

[d] *Institute of Chemistry, Academia Sinica, Nankang, Taipei, Taiwan*

Abstract: *A series of hybrid Aldimine-type Schiff base derivatives including trimethoxyphenyl ring and 1,2,4-triazle-3-thiol/thione were designed as tubulin inhibitors. The molecular docking simulations on tubulin complex (PDB: 1SA0) revealed that derivatives with nitro and /or chloro or dimethylamine substitutes (4-Nitro, 2-Nitro, 3-Nitro, 4-Cl-3-nitro, and 4-N(CH_3)$_2$) on the aldehyde ring were the best compounds with remarkable binding energies (-9.09, -9.07, -8.63, -8.11, and -8.07 kcalmol^{-1}, respectively) compared to Colchicine (-8.12 kcalmol^{-1}). These compounds were also showed remarkable binding energies from -10.66 to -9.79 and -10.12 to -8.95 kcalmol^{-1} on human (PDB: 1PD8) and Candida albicans (PDB: 3QLS) DHFR, respectively. The obtained results of cytotoxic activities against HT1080, HepG2, HT29, MCF-7, and A549 cancer cell lines indicated that 4-Nitro and 2-Nitro substituted compounds were the most effective agents by mean IC_{50} values of 11.84±1.01 and 19.92±1.36 μM, respectively. 4-Nitro substituted compound (5 μM) and 2-Nitro substituted compound (30 μM) were able to strongly inhibit the tubulin polymerization compared to Colchicine (5 μM) and 4-Nitro substituted compound displayed IC_{50} values of 0.16±0.01 μM compared to that of colchicine (0.19±0.01 μM). This compound also showed the lowest MIC values on all tested microbial strains including three Gram-positive, four Gram-negative, and three yeast pathogens.*

Keywords: *Schiff bases • Heterocycles • Antitumor agents • Molecular modelling • Antimicrobial*

Introduction

Combretastatin A-4 (CA-4) (Figure 1), a natural product originated from the bark of South African willow tree Combretum caffrom, belongs to the family of microtubule targeting agents (MTA) which exhibits strong growth suppression toward a wide range of human tumors including multidrug resistant (MDR) cancer at nanomolar concentrations [1-3]. During the two last decades many structure-activity relationship (SAR) studies have been performed to synthesize more potent analogs of CA-4 by modification or derivatization of C=C bond, or the aromatic rings A and B (Figure 1) [4-6].

Most of the recently published articles mentioned that alteration of 3,4,5-trimethoxy phenyl group (TMP, ring A) of CA-4 negatively affected the antimitotic activity [7-9]. In fact, the TMP group is the characteristic main ring of CA-4, Colchicine, and Podophyllotoxin (Figure 1), accommodated to the hydrophobic pocket in the colchicine site of tubulin [7, 10]. Colchicine and its derivatives as well as N-deacetyl-N-(2-mercaptoacetyl)-colchicine, DAMA-colchicine (the main tubulin ligand of PDB code 1SA0) (Figure 1), shows H-bonding contacts between methoxy group of TMP ring and Cysβ241 as critical residues in the colchicine binding site (CBS) [11-13]. The common pharmacophore models for colchicine binding inhibitors (CBIs) are including i) Nguyen model (three hydrogen bond acceptors (A1, A2, and A3), one hydrogen bond

*donor (D1), two hydrophobic centers (H1 and H2), and one planar group (R1)); in this model residues of Cysβ241, Leuβ252, Aspβ251, Alaβ250, and Valα181 were introduced as hydrogen bond acceptors [14, 15], ii) Niu model (one hydrogen bond acceptor (HBA), one hydrogen bond donor (HBD), one hydrophobic feature (HY), and one ring aromatic feature (RA)) in which Asnα101 was introduced as HBA [13], and iii) Da model consisted of three hydrogen bond acceptors (including Valα181, Leuβ252, and Cysβ241), a hydrogen bond donor (Thrα179), and a hydrophobic skeleton with four hydrophobic centers. It should be noted that the two last mentioned models were relatively derived from the first model (Nguyen model) [16]. The critical role of this biologically active pharmacophore, TMP, not only identified for combretastatin derivatives (via fitting to β-tubulin pocket) but also reported for a dozens of compounds exhibited diverse biological activities [1, 7]. For example, Jeong et al. designed a series of heat shock protein (hsp90) inhibitors via connecting the TMP ring of PU3 (Figure 1) and resorcinol ring of VER-49009 (Figure 1) to combat against gefitinib-resistant cell line of H1975 [17]. The obtained results showed that the designed hybrid molecule (**1**) (Figure 1) was able to efficiently suppress the expression of the both hsp90 and endothelial growth factor receptor (EGFR) [17]. Furthermore, the TMP group is also present in the structure of Trimetrexate and Trimethoprim (Figure 1) identified as one of the most important inhibitor of human and prokaryotic dihydrofolate reductase (DHFR), respectively [18]. In addition, the TMP ring exhibited the key role in the structure of many synthesized compounds evaluated for antimicrobial, anti-HIV (by inhibition of reverse transcriptase activity), and anti-leishmanial activity [19-21].*

The chemistry of 1,2,4-triazole derivatives has gained broad attention due to their diverse biological activities such as anticancer, antimycotic, antimalarial, and antitubercular as well as antiparasitic, herbicidal, analgesic, CNS stimulant, antianxiety, and antimigraine activities (Rizatriptan) (Figure 1) [22-25]. The Aldimine-type Schiff bases of 1,2,4-triazole which successfully synthesized by Li et al. exhibited considerable in vitro antitumor potencies against the both human liver cancer cell line (Bel-7402) and breast adenocarcinoma cells (MCF-7) [26]. This pharmacophore (Aldimine-type Schiff base) has been also found in the structure of many well-known antibacterial drugs like Nitrofurantoin, Nitrofurazone, and Furazolidone (Figure 1) [27]. Ganguly et al. reviewed the potential role of various metal chelates of the Schiff base N-(2-hydroxy acetophenone) glycinate for overcoming formation of multi-drug resistance tumors via different mechanisms such as deactivating the c-Raf-1 kinase and c-Ha-ras signalling pathway [28].

Bearing in mind the above mentioned facts regarding the biological activities of 1,2,4-triazole-3-thiol/thione derivatives, Schiff bases, and noticeable properties of TMP ring, the present study was undertaken to design some novel Aldimine-type Schiff base derivatives of 4-amino-5-(3,4,5-trimethoxybenzyl)- 1,2,4-triazole-3-thiol/thione as Hybrid pharmacophore structure (Scheme 1) as anti-tubulin agents based on the molecular docking simulation against tubulin CBS followed by synthesis of the best compounds according to the binding energies and effective interactions with CBS of tubulin. In addition, docking simulations were also performed on other protein targets including human DHFR (hDHFR), hsp90, vascular endothelial growth factor receptor 2 (VEGFR2), Staphylococcus aureus and Candida albicans DHFR. Finally, the cytotoxic and anti-tubulin activities as well as antimicrobial effects of the synthesized derivatives were evaluated.

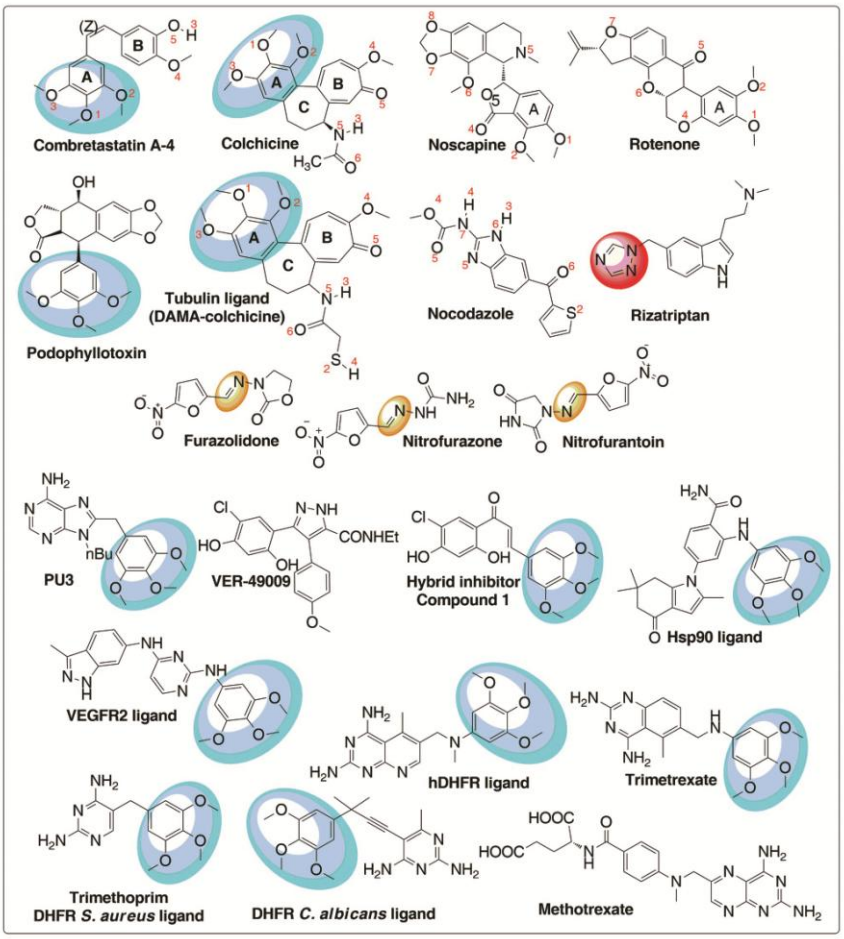

Figure 1. *The structures of tubulin inhibitors (Combretastatin A-4, Colchicine, Podophyllotoxin, Noscapine, Nocodazole, and Rotenone), main ligand of the docking protein targets, and other structures explained in Introduction section, (numbering of atoms in above structures was carried out in order to avoid confusing of realizing the molecular docking results).*

Results and discussion

Molecular docking

In the present study, hybrid pharmacophore structures comprising TMP, 1,2,4-triazole-3-thiol/thione, and Aldimine-type Schiff base were designed in order to introduce novel anti-tubulin agents mimic CA-4 and Colchicine via interaction with CBS of αβ-tubulin heterodimer. Initially, the molecular docking simulation has been carried out with the X-ray crystal structure of tubulin-colchicine: stathmin-like domain complex (PDB code: 1SA0) and interactions between compounds and CBS were reported. In parallel, other protein targets with TMP-containing main ligand including hDHFR (PDB code: 1PD8), hsp90 (PDB code: 3MNR), and VEGFR2 (PDB code: 3CJF) were also selected for molecular docking evaluations. Forty eight Aldimine-type Schiff base structures (the compounds **A-01** *to* **A-24** *as E isomers and the compounds* **A-25** *to* **A-48** *as Z isomers) (Scheme 1) were included in the docking studies for all above mentioned protein targets. These compounds were classified in 3 main groups: i) compounds bearing hydroxyl, methoxy and ethoxy groups, mimicking the B ring of colchicine and CA-4, ii) structures with nitro moiety, a hydrogen bond acceptor with electron withdrawing effect [29] and iii) compounds with 4-N(CH$_3$)$_2$ group substituted on the B ring as well as the B-ring unsubstituted derivatives (Scheme 1).*

*a) Tubulin: The obtained results of interaction between tubulin and the designed compounds (Aldimine-type Schiff bases and compound (***2***), standard inhibitors (Colchicine, Noscapine, Rotenone, Nocodazole and CA-4), and DAMA-colchicine are shown in Table 1. Because of various hydrogen bond acceptor in pharmacophore models for CBIs [13-16] and critical role of TMP ring for anti-tubulin agents [2] in this study hydrogen bond interaction between Cysβ241 and methoxy groups in TMP ring together with favorable binding energies were considered to select the most suitable compounds. The results of docking study were categorized according to the binding energies and cluster ranks. The first and second cluster ranks of DAMA-colchicine were found to be the interaction between TMP ring and Cysβ241 by binding energies of -8.2 and -8.1 kcalmol^{-1}, respectively, while Colchicine showed the same interaction with binding energy of -8.12 kcalmol^{-1} in its first cluster rank.*

Therefore, in the case of the designed compounds only the clusters with binding energy up to -8.1 kcalmol^{-1} were reported (ranking energy 1 to 41 in Table 1).

The compounds with hydroxyl, methoxy and ethoxy moieties mimic B ring of CA-4 and Colchicine; the group i, did not display appropriate binding energy with tubulin in CBS. In the first category of this group, compounds with 3-OH-4-OCH$_3$ moiety, H-Bond interaction was observed between Cysβ241 and TMP ring by binding energies range of -8.01 to -7.35 kcalmol^{-1} which was not as good as DAMA-colchicine (-8.2 kcalmol^{-1}). In the case of the second category, 4-OH-3,5-diOCH$_3$ substituted compounds, only the thione tautomer in the both E and Z isomeric forms of them exhibited this interaction by binding energy of -7.69 and -7.07 kcalmol^{-1} for compounds **A-26** *and* **A-02**, *respectively. Among compounds with 3-OC$_2$H$_5$-4-OH moiety, the third category, only compound* **A-03** *(E isomer of thione form) interacted with this residue by TMP ring by ΔG of -7.32 kcalmol^{-1}. The fourth (3,4-diC$_2$H$_5$ substitute) and the fifth (3-OCH$_2$O-4 substitute) categories of group i displayed new style of interactions; the structures in the compounds* **A-04**, **A-16**, *and* **A-17** *were completely flip flapped and their B ring substitutes exhibited H-bond interaction with Cysβ241 while their TMP ring interacted with Asnα101, Serα178, and Asnα101 by binding energies of -7.93, -8.35, and -8.19 kcalmol^{-1}, respectively. So, the last mentioned categories were not selected for synthesis step because the TMP ring was not involved in the H-bond interaction with Cysβ241 in theses conformers (Table 1).*

As presented in Table 1, the compounds of group ii were the best compounds based on their binding energy ranks. The first cluster of compound **A-30**, *bearing 4-OCH$_3$-3-nitro group on B ring, was not displayed H-bonding with Cysβ241 while O atom of nitro group interacted with NH moiety of Glyα144 (1.819 Å) (binding energy of -8.38 kcalmol^{-1}) (Table 1). The second cluster rank of this compound represented H-bond between Cysβ241 and TMP ring by binding energy of -7.4 kcalmol^{-1}. The E isomer of this compound,* **A-06**, *displayed such interaction in the first cluster rank by ΔG of -7.43 kcalmol^{-1} but none of Z and E isomer of the thiol tautomeric forms of this category (bearing 4-OCH$_3$-3-nitro group on B ring) in the first cluster rank exhibited this interaction and also favorable binding energy (-7.85 and -7.94 kcalmol^{-1}, respectively). In the second category of group ii, the 2-nitro substituted,* **A-19** *displayed the first H-bond interaction between Cysβ241 and TMP ring by binding energy of -8.57 kcalmol^{-1} in its 4th cluster rank compared to Colchicine and DAMA-colchicine (-8.12 and -8.2 kcalmol^{-1}, respectively) (Table 1) (Figure 2a). It should be noted that the first cluster rank of this compound (***A-19***), the second order of rank energy, exhibited H-bond interactions between thiol group and Leuβ248 (2.001 Å), N3 atom of C ring with Alaβ250 (1.881 Å), and nitro group with Glyα144 (2.218 Å) by binding energy of -9.07 kcalmol^{-1}, while the TMP ring was near to Leuβ248 and Lysβ254 (Table 1) (Figure 2b). In the thione form of this compound (***A-07***), placed at 29th rank by binding energy of -8.3 kcalmol^{-1}, the TMP ring was surrounded by Cysβ241, Leuβ248, Leuβ255, and Alaβ250 while nitro group of B ring and N2 atom of C ring interacted with Glyα144 (2.033 Å) and Alaβ250 (2.034 Å), respectively (Table 1). The Z isomers of this category (compounds* **A-43** *and* **A-31***) placed at 4th and 6th rank of binding energies (-9.00 and -8.97 kcal/mol, respectively), did not display interaction between Cysβ241 and TMP ring (Table 1). The first cluster rank of 3-nitro substituted compounds (***A-44***, ***A-08***, ***A-20***, and* **A-32***), the third category of group ii, exhibited docking energies in the range of -8.69 to -8.26 kcalmol^{-1} but did not display H-bonding with Cysβ241 (Table 1). This category was selected for synthesis step because of favorable binding energy. However, the TMP ring of these compounds interacted with Cysβ241 by binding energies of -7.73, -7.23, -7.57, and -7.65 kcalmol^{-1}, respectively. The fourth category of group ii, the 4-nitro substituted, was the best category according to their binding energy. The compound* **A-21** *was taken the first energy rank (-9.09 kcalmol^{-1}); this conformer interacted with Glyα144 and Glnβ247 by nitro and thiol group, respectively while the TMP ring was buried into hydrophobic pocket (Leuβ255, Alaβ250, Leuβ248) of CBS (Table 1) (Figure 2c). Its thione form,* **A-09**, *displayed these interactions (except for H-bond between SH group) by binding energy of -8.75 kcalmol^{-1}, and also showed π-cation interaction between the B ring and Lysβ254 (Table 1). The Z isomer of this compound,* **A-33**, *was placed in the third rank of energy (binding energy of -9.01 kcalmol^{-1}) (Table 1). The compound* **A-45** *exhibited π-cation interaction between Lysβ254 and B ring, and also H-bond interaction between nitro and thiol group with Glyα144 and Serα178, respectively (binding energy of -8.88 kcalmol^{-1}) (Table 1). In the last category of group ii, the 4-chloro-3-nitro substituted, in the both of E isomeric forms (compounds* **A-10** *and* **A-22***) the TMP ring interacted with Cysβ241 (the first cluster rank) by docking energies of -8.11 and -7.96 kcalmol^{-1}, respectively (Table 1). However, the Z isomeric forms of them,* **A-34** *and* **A-46**, *exhibited such interaction in the 4th and 5th cluster ranks by binding energies of -7.73 and -7.53 kcalmol^{-1}, respectively. To sum up, in this group, H-bond interaction between Glyα144 and nitro substitutes were observed in compounds with favorable binding energies (***A-21***, ***A-19***, ***A-33***, ***A-43***, ***A-31***, ***A-45***, ***A-09***, ***A-20***, ***A-30***, and* **A-07***) in the range of -9.09 to -8.3 kcalmol^{-1} (Table 1). The same results were reported by Zhao et al. who observed that the most potent tubulin polymerization inhibitor interacted with Glyα144 via hydrogen bond in CBS [30]. This interaction was also reported for other tubulin inhibitor agents [29].*

*Although in the first category of group iii, bearing 4-N(CH$_3$)$_2$, all compounds (***A-11***, ***A-23***, ***A-35***, and* **A-47***) exhibited H-bond interaction between TMP ring and Cysβ241 in CBS by binding energies of -8.07, -7.85, -7.48, and -7.74 kcalmol^{-1}, respectively, only* **A-11** *displayed binding energy higher than -8.00 kcalmol^{-1} (Table 1). In the second category of this group, only the first cluster of thione forms (compounds* **A-36** *and* **A-12***) displayed H-bond interaction between Cysβ241 and TMP ring by binding energies of -7.64 and -7.38 kcalmol^{-1}, respectively. Therefore, none of the compounds in this category were suitable for synthesis step.*

To sum up, the 4-Cl-3-nitro, 2-, 3-, and 4-nitro and 4-dimethylamine substituted benzaldehydes were used for synthesis of Aldimine-type Schiff base derivatives.

The molecular simulation results of compound **2** *revealed the H-bonding interaction between Cysβ241 in CBS and TMP at cluster rank 2 (thione form,* **Tn***) and cluster rank 1 (thiol form,* **Tl***) by binding energies of -5.48 and -5.89 kcalmol^{-1}, respectively.*

Total rank of binding energy for all designed compounds, standard inhibitors, and DAMA-colchicine was 650 levels among which the worst binding energy of Aldimine-type Schiff bases and compound **2** *belonged to the cluster rank 90 (***A-14***) and 28 (***Tn***) with binding energy of -5.15 and -4.84 kcal/mol, respectively. All of the Aldimine-type Schiff bases exhibited well binding energy compared to CA-4 in their first cluster ranks while the docking binding energies of all selected compounds for synthesis were better than Noscapine, Rotenone, Nocodazole and CA-4 (Table 1).*

Table 1. *Top rank of AutoDock binding energy (up to -8.1 kcalmol-1) between Colchicine binding site of tubulin (PDB code: 1SA0) and designed compounds main ligand, and standard inhibitors.*

Rank[a]	Compound	Cluster Rank[b]	ΔG[c] (kcal/mol)	K_i[d] (μM)	H-Bonding[e] (distance, Å)
1	A-21	1	-9.09	0.22	β: Gln247: O -- H2 (2.093) α: Gly144: HN -- O1-Nitro(1.795)
2	A-19	1	-9.07	0.23	β: Leu248: O -- H2 (2.001) β: Ala250: HN -- N3 (1.881) α: Gly 144: HN -- O2 -Nitro (2.218)
3	A-33	1h	-9.01	0.25	α: Gly144: HN -- O2-Nitro (1.821)
4	A-43	1	-9	0.25	β: Gln247: O -- H2 (1.948) α: Gly144: HN -- O2-Nitro (1.777)
5	A-19	2	-8.98	0.26	β: Leu248: O -- H2 (1.987) β: Ala250: HN -- N3 (1.858) α: Gly144: HN -- O1-Nitro(1.808)
6	A-31	1	-8.97	0.27	α: Gly144: HN -- O1-Nitro(1.796)
7	A-45	1[h]	-8.88	0.31	α: Ser178: O -- H2 (2.146) α: Gly144: HN -- O2-Nitro (1.863)
8	A-21	2	-8.86	0.32	β: Gln247: O -- H2 (2.202) α: Gly144: HN -- O2-Nitro (1.731)
9	A-33	2	-8.83	0.34	α: Ser178: O -- H1(1.996) α: Gly144: HN -- O1-Nitro(1.876)
10	A-09	1	-8.75	0.39	α: Gly144: HN -- O1-Nitro(1.806)
11	A-34	1	-8.7	0.42	α: Val181: HN -- O2-Nitro (2.031) β: Cys241: HG -- N2 (2.107)
12	A-44	1	-8.69	0.43	β: Leu248: O -- H2 (2.018) α: Gly144: HN -- O1-Nitro(1.798)
13	A-08	1	-8.63	0.47	α: Gly144: HN -- O1-Nitro(1.768)
14	A-46	1	-8.63	0.48	β: Ala317: O -- H2 (1.992) α: Val181: HN -- O2-Nitro (2.183)
15	A-08	2	-8.62	0.48	α: Gly144: HN -- O2-Nitro (1.746)
16	A-21	3	-8.61	0.49	β: Gln247: O -- H2 (2.107) α: Gly144: HN -- O2-Nitro (1.807)
17	A-09	2	-8.6	0.49	α: Gly144: HN -- O2-Nitro (1.677)
18	A-09	3	-8.58	0.51	α: Gly144: HN -- O2-Nitro (1.732) α: Ser178: HG -- N2 (1.973)

19	A-19	4	-8.57	0.52	α: Val181: HN -- O1-Nitro(1.944) β: Lys352: HZ -- O2-Nitro (2.078) β: Cys241: HG -- O2 (2.173)
20	A-21	4	-8.56	0.53	α: Gly144: HN -- O2-Nitro (1.792) α: Ser178: HG -- N2 (2.203) β: Gln247: O -- H2 (2.116)
21	A-20	1	-8.53	0.56	α: Gly144: HN -- O2-Nitro (1.719)
22	A-21	5	-8.5	0.59	α: Gly144: HN -- O1-Nitro(1.814) α: Ser178: HG -- N2 (1.935)
23	A-09	4	-8.47	0.62	α: Gly144: HN -- O1-Nitro(1.785)
24	A-20	3	-8.39	0.71	α: Ala250: HN -- O2 (2.217) β: Lys352: HZ -- O2-Nitro (1.895) α: Val181: HN -- O1-Nitro(2.003) β: Cys241: HG -- N3 (2.050)
25	A-30	1	-8.38	0.72	α: Gly144: HN -- O2-Nitro (1.819)
26	A-45	4	-8.38	0.72	α: Gly144: HN -- O2-Nitro (1.835)
27	A-19	5	-8.35	0.76	α: Val181: HN -- O1-Nitro(1.772) β: Lys352: HZ -- O2-Nitro (1.856) β: Cys241: HG – O1 (1.98)
28	A-16	1	-8.35	0.76	β: Asn258: O -- H2 (2.079) β: Cys241: HG -- O (3-OEt) (1.979) α: Ser178: HG -- O1 (1.793)
29	A-07	1	-8.3	0.83	α: Gly144: N -- O2-Nitro (2.033) β: Ala250: HN -- N2 (2.034)
30	A-32	1	-8.26	0.88	α: Gly144: HN -- O1-Nitro(1.754) α: Ser178: HG -- O3 (2.146)
31	A-07	2	-8.26	0.89	β: Lys352: HZ -- O1-Nitro(1.94) β: Cys241: HG -- O2 (2.155)
32	A-16	2	-8.25	0.90	α: Val181: HN -- O2-Nitro (1.985) α: Asn101: HD -- O1 (2.244)
33	A-16	3	-8.22	0.94	α: Ser178: HG -- O3 (2.213) α: Val181: HN -- N2 (2.171) β: Cys241: HG -- O (3-OEt) (1.977)
34	DAMA-colchicine[h]	1	-8.2	0.98	α: Thr179: O (2.013) -- H4 β: Cys241: HG -- O1 (1.889)
35	A-17	1	-8.19	1.00	β: Cys241: HG -- O (4-OEt) (2.181) α: Val181: HN -- N3 (2.085) α: Asn101: HD -- O3 (1.996)
36	A-07	3	-8.15	1.07	β: Lys352: HZ -- O2-Nitro (1.918) β: Cys241: HG -- O1 (1.9) α: Val181: HN -- O2-Nitro (2.212)
37	A-08	4	-8.12	1.12	α: Gly144: HN -- O2-Nitro (2.129)
38	Colchicine	1	-8.12	1.11	β: Cys241: HG -- O1 (1.956)
39	A-10	1	-8.11	1.14	α: Val181: HN -- O2-Nitro (1.826) β: Cys241: HG -- O1 (2.139)
41	A-11	1	-8.07	1.21	β: Cys241: HG -- O1 (1.956)

42	Noscapine	1	-8.07	1.21	α: Asn101: HD -- O8 (2.144) β: Cys241: HG -- O2 (1.829)
44	Rotenone	1[g]	-8.00	1.37	β: Ala250: HN -- O4 (2.211) β: Lys254: HZ -- O1 (2.015)
66	Nocodazole	1	-7.81	1.87	α: Asn101: HD -- O5 (1.906) α: Thr179: O -- H3 (2.187)
343	CA-4	1	-6.86	9.44	α: Val181: HN -- O5 (2.11) β: Cys241: HG -- O3 (2.049)

[a] *Sorting based on binding energy;* [b] *No. of cluster;* [c] *Estimated ΔG binding;* [d] *Estimated inhibition constant, K_i (μM);* [e] *Chain: residue with H-bonding: group -- atom no. (distance, Å);* [f] *Residues without H-bonding near TMP ring in hydrophobic pocket;* [g] *π-cation interaction between B-ring and Lysβ254;* [h] *N-deacetyl-N-(2-mercaptoacetyl)-colchicine, the main ligand in tubulin (PDB code: 1SA0).*

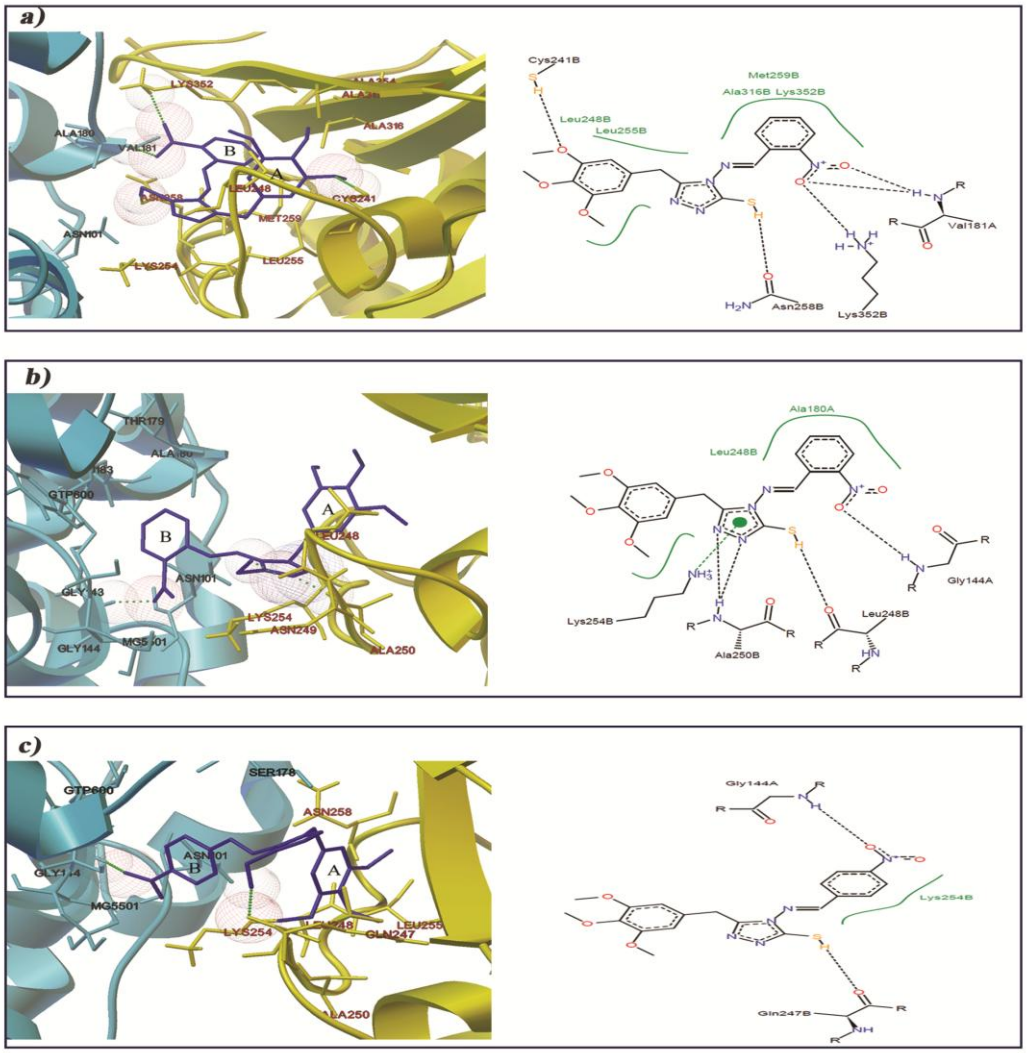

Figure 2. *Interactions of compounds in colchicine binding site (CBS) of αβ-tubulin (PDB code: 1SA0). Left: 3D-view, The α and β chains were showed in turquoise and yellow color, respectively. Residues labels of α chain and β chain indicated by black and red color, respectively. H-bonding interaction were showed by green dots and wired spheres. a) blue structure, the first conformer of 1st cluster rank of* **A-21**; *b) blue structure, the first conformer of 1st cluster rank of* **A-19**; *c) blue structure, the first conformer of 4th cluster rank of* **A-19**; *Right: 2D-view, Black dashed lines indicate hydrogen bonds, salt bridges, and metal interactions. Green solid line show hydrophobic interactions and green dashed lines show π-π and π-cation interactions, the figure created by The ProteinPlus Webserver http://poseview.zbh.uni-hamburg.de/pdb_files.*

b) DHFR

-hDHFR: The molecular docking studies for all of Schiff base derivatives were performed and the output docking files (.dlg file) ranked based on binding energies. Analyses of docking results were reported based on the first 22 ranking binding energies of 48 designed compounds, main protein ligand (2,4-diamino-5-methyl-6-[(3,4,5-trimethoxy-N-methylanilino)methyl]pyrido[2,3-d]pyrimidine) and standard inhibitors (Trimetrexate, Methotrexate and Trimethoprim). The compound **A-10**, *4-chloro-3-nitro B ring substituted in E thione isomeric form, was the best structure according to the binding energy (-10.66 kcalmol^{-1}) comparted to the main protein ligand, Trimetrexate, Methotrexate, and Trimethoprim (-9.75, -9.4, -9.31, and -7.81 kcalmol^{-1}, respectively and binding energy rank of 22, 52, 66, and 331, respectively) (Table 2). The best conformer of this compound exhibited H-bond interaction between nitro group and Glnα35 (2.103 Å) (Figure S-1a, see the Supplementary Material). Its TMP ring showed π-π interaction with Tyrα121 and NDP300 (NADPH dihydro-nicotinamide-adenine-dinucleotide phosphateand) and also Tyrα121 displayed such interaction with C ring of this compound while the main ligand exhibited only π-π interaction between TMP ring and Pheα31 (Figure S-1b, see the Supplementary Material). The TMP ring of compound* **A-10** *was almost overlaid on pyrido[2,3-d]pyrimidine ring of the main ligand while two structures were completely flip flapped in the active site of hDHFR (Figure S-1a and Figure S-1b, see the Supplementary Material).*

In conclusion, the selected compounds of the previous section (compounds with 4-Cl-3-nitro, 2-, 3-, and 4-nitro substituted) were exhibited appropriate binding energies against hDHFR (18 of 24 cluster rank) and even better than the main ligand, Trimetrexate, Methotrexate and Trimethoprim (Table 2).

-Microbial DHFR: According to the above obtained docking results and also the presence of the 1,2,4-triazole moiety in the structure of designed compounds, the microbial protein targets (DHFR from S. aureus, PDB code: 2W9S and C. albicans, PDB code: 3QLS) were added to the docking studies. All of structures were showed better binding energies compared to Trimethoprim against the both applied protein targets (binding energy of -7.59 and -7.12 kcalmol^{-1} against DHFR from S. aureus and C. albicans, respectively).

The compound **A-01** *represented H-bond interaction between NH moiety in C ring and Serα49 (1.868 Å), OH group in B ring with Pheα92 (2.189 Å), and OCH_3 moiety in TMP ring with Hisα23 (2.043 Å) by binding energy of -9.57 kcalmol^{-1} against DHFR from S. aureus (Figure S-1c). In addition, this compound displayed π-π interaction between C ring and Pheα92 (Figure S-1c, see the Supplementary Material). Alike compound* **A-01**, *the best conformer of compound* **A-10** *was also displayed all of the mentioned interactions except for interaction of OH group in B ring with Pheα92 (Figure S-1d, see the Supplementary Material).*

The molecular docking results of C. albicans DHFR were better than S. aureus target (Table 3). The compound **A-22**, *thiol form of* **A-10**, *displayed the highest binding energy (-10.12 kcalmol^{-1}) compared to Trimetrexate, main ligand, Methotrexate and Trimethoprim (C. albicans DHFR binding energies of-9.03, -8.83, -8.18, and -7.12 kcalmol^{-1}, respectively and binding energy rank of 19, 29, 58, and 272, respectively). In addition to H-bond interaction with Serα61 which observed in the main ligand and standard inhibitors, this compound (***A-22***) represented two additional H-bond interactions with Argα72 and nitro group as well as π-π interaction between Pheα36 and TMP ring like Trimetrexate (Quinazoline ring) (Figure S-1e and Figure S-1f, see the Supplementary Material). Consequently, the compounds* **A-22**, **A-20**, **A-10**, **A-08**, *and* **A-09** *(previously selected in the tubulin section) were found to be more efficient than the main ligand, Methotrexate and Trimethoprim against C. albicans DHFR (Table 3).*

Table 2: *Top rank of AutoDock binding energy (the first 22 clusters) between other three protein targets and designed compounds/ main protein target ligands/ standard inhibitors.*

	hDHFR **(1PD8)**			***hsp90*** **(3MNR)**			***VEGFR-2*** **(3CJF)**		
Rank[a]	**Compound**	**Clu.**[b]	**ΔG**[c]	**Compound**	**Clu.**	**ΔG**	**Compound**	**Clu.**	**ΔG**
1	*A-10*	*1*	*-10.66*	*Ligand*[d]	*1*	*-13.14*	*Ligand*[e]	*1*	*-8.93*
2	*A-22*	*1*	*-10.6*	*A-34*	*1*	*-9.6*	*Ligand*	*2*	*-8.3*
3	*A-08*	*1*	*-10.46*	*Ligand*	*2*	*-9.59*	*A-45*	*1*	*-8.12*
4	*A-22*	*2*	*-10.16*	*Ligand*	*3*	*-9.53*	*Ligand*	*4*	*-8.04*
5	*A-06*	*1*	*-10.15*	*A-20*	*1*	*-9.39*	*A-42*	*1*	*-7.98*
6	*A-10*	*2*	*-10.15*	*Ligand*	*4*	*-9.39*	*A-22*	*1*	*-7.95*
7	*A-18*	*1*	*-10.15*	*A-32*	*1*	*-9.25*	*A-20*	*1*	*-7.88*
8	*A-10*	*3*	*-10.10*	*A-18*	*1*	*-9.25*	*A-44*	*1*	*-7.87*
9	*A-20*	*1*	*-10.00*	*A-06*	*1*	*-9.15*	*A-20*	*2*	*-7.83*
10	*A-22*	*3*	*-9.98*	*A-10*	*1*	*-9.11*	*A-34*	*1*	*-7.71*
11	*A-20*	*2*	*-9.90*	*A-18*	*1*	*-9.09*	*A-22*	*2*	*-7.68*
12	*A-22*	*4*	*-9.88*	*A-08*	*1*	*-9.07*	*A-18*	*1*	*-7.67*

13	A-21	1	-9.86	A-08	2	-9.07	A-20	4	-7.65
14	A-17	1	-9.86	A-46	1	-9.07	A-32	1	-7.6
15	A-08	2	-9.83	A-14	1	-9.06	A-45	2	-7.6
16	A-18	2	-9.83	A-18	2	-9.03	A-46	1	-7.59
17	A-06	2	-9.82	A-18	3	-8.94	A-30	1	-7.53
18	A-05	1	-9.82	A-16	1	-8.92	A-21	1	-7.5
19	A-19	1	-9.82	A-34	2	-8.9	A-34	2	-7.45
20	A-09	1	-9.81	A-30	1	-8.88	Ligand	5	-7.45
21	A-10	4	-9.79	A-20	2	-8.88	A-07	1	-7.43
22	Ligand[f]	1	-9.75	A-44	1	-8.87	A-33	1	-7.42

[a] Sorting based on binding energy; [b] No. of cluster; [c] Estimated ΔG binding (Kcalmol^{-1}); [d] 2-[(3,4,5-trimethoxyphenyl)amino]-4-(2,6,6-trimethyl-4-oxo-4,5,6,7-tetrahydro-1H-indol-1-yl)benzamide, main ligand of hsp90 (PDB code: 3MNR); [e] N4-(3-methyl-1H-indazol-6-yl)-N2-(3,4,5-trimethoxyphenyl)pyrimidine-2,4-diamine, main ligand of VEGFR-2 (PDB code: 3CJF); [f] 2,4-Diamino-5-methyl-6-[(3,4,5-trimethoxy-N-methylanilino)methyl]pyrido[2,3-d]pyrimidine, main ligand of hDHFR (PDB code 1PD8).

Table 3: *Top rank of AutoDock binding energy (the first 22 clusters) between two microbial protein targets with designed compounds/ main protein target ligands/standard inhibitors.*

	DHFR* (2W9S)** ***S. aureus			***DHFR* (3QLS)** ***C. albicans***		
Rank[a]	**Compound**	**Clu.[b]**	**ΔG[c]**	**Compound**	**Clu.**	**ΔG**
1	A-01	1	-9.57	A-22	1	-10.12
2	A-05	1	-9.52	A-20	1	-9.83
3	A-27	1	-9.47	A-10	1	-9.8
4	A-39	1	-9.38	A-15	1	-9.62
5	A-01	2	-9.34	A-10	2	-9.56
6	A-10	1	-9.31	A-14	1	-9.53
7	A-13	1	-9.31	A-18	1	-9.44
8	Methotrexate	1	-9.23	A-08	1	-9.42
9	A-09	1	-9.2	A-20	2	-9.37
10	A-05	2	-9.15	A-22	2	-9.35
11	A-01	4	-9.14	A-22	3	-9.34
12	A-01	5	-9.14	A-08	2	-9.33
13	A-17	1	-9.08	A-10	3	-9.27
14	A-44	1	-9.07	A-22	4	-9.26
15	A-06	1	-9.03	A-06	1	-9.24
16	A-27	2	-9.03	A-06	2	-9.18
17	A-21	1	-9.03	A-18	2	-9.09
18	A-11	1	-9.01	A-06	3	-9.03
19	A-05	3	-8.93	Trimetrexate	1	-9.03
20	A-32	1	-8.92	A-08	3	-9.02
21	A-38	1	-8.91	A-22	5	-9
22	A-22	1	-8.9	A-09	1	-8.99
29				Ligand[d]	1	-8.83

[a] Sorting based on binding energy; [b] No. of cluster; [c] Estimated ΔG binding (Kcalmol^{-1}); [d] 6-

methyl-5-[3-methyl-3-(3,4,5-trimethoxyphenyl)but-1-yn-1-yl]pyrimidine-2,4-diamine, main ligand of C. albicans DHFR (PDB code: 3QLS); [e]The main ligand of S. aureus DHFR (PDB code:2W9S)

c) Hsp90 and VEGFR2: The hsp90 and VEGFR2, as additional protein targets, were also selected and all designed Schiff bases were subjected to simulation using the similar method described for hDHFR. The molecular docking results was reported based on the first 22 ranking binding energies of 48 designed compounds and the main protein ligands. In the case of the both targets (hsp90 and VEGFR2), main ligands exhibited the highest binding energies (-13.14 and -8.93 kcalmol^{-1}, respectively) (Table 2).

The O atoms of nitro group in the compound **A-34,** *the best compound against hsp90 by binding energy of -9.6 kcalmol^{-1}, interacted with H atom of crystallographic water and Lysα58 in hsp90 active site, in addition to its NH moiety of C ring which interacted by another crystallographic water while the TMP ring showed π-π interaction with Pheα138 (Figure S-2a, see the Supplementary Material). The interactions of the second compound,* **A-20***, were including H-bonds between thiol (C ring) and methoxy (TMP ring) moiety with crystallographic waters and also nitro group of B ring with Lysα58 by distances of 2.179, 2.241, and 2.188 Å, respectively (Figure S-2b, see the Supplementary Material). The crystallographic water molecules in the active site of hsp90 interacted with carbonyl groups and NH_2 moiety of the main ligand; while methoxy groups in the TMP ring and NH_2 moiety interacted with Lysα58 (H-bond and π-cation interactions) and Aspα93, respectively (Figure S-2c, see the Supplementary Material).*

The compound **A-45** *exhibited higher binding energy (-8.12 kcalmol^{-1}) for VEGFR2 compared to other compounds by H-bond interactions including nitro group with Asnα921 (2.225 and 1.86 Å), N atom of C ring with Cysα917 (1.827 Å), and the methoxy moiety of TMP ring with CSO1043 (L-peptide linking, 1.907 Å) (Figure S-2d, see the Supplementary Material) while the main ligand interacted by N atom of its pyrimidine ring with Cysα917 (2.006 Å) (Figure S-2e, see the Supplementary Material). The TMP ring of compound* **A-22** *was almost overlaid on the same ring of the main ligand and this compound showed H-bond interactions by methoxy, N atom of C ring, and nitro group of B ring with Asnα921 (2.06 Å), Cysα917 (2.049 Å), and CSO1043 (1.715 Å), respectively, and also exhibited π-π interaction between Pheα916 and its C ring (Figure. S-2f, see the Supplementary Material).*

*To sum up, the compounds bearing 2-, 3-, 4-nitro, 4-chloro-3-nitro group on B ring (***A-21***,* **A-19***,* **A-33***,* **A-43***,* **A-31***,* **A-45***,* **A-09***,* **A-34***,* **A-44***,* **A-08***,* **A-46,** *and* **A-10** *for tubulin;* **A-10***,* **A-22***,* **A-08***,* **A-20***,* **A-21***,* **A-19***,* **and A-09** *for hDHFR;* **A-10***,* **A-09***,* **A-44***,* **A-21***,* **A-32***,* **A-22***, and* **A-34** *for S. aureus DHFR;* **A-22***,* **A-20***,* **A-10***,* **A-08***,* **A-09***, and* **A-34** *for C. albicans DHFR;* **A-34***,* **A-20***,* **A-32***,* **A-10***,* **A-08***, and* **A-46** *for hsp90; and* **A-45***,* **A-22***,* **A-20***,* **A-44***,* **A-34** *for VEFGR2) (Table 1, Table 2, and Table 3) were the most effective derivatives based on the molecular simulation results. Furthermore, their E isomeric forms exhibited better docking results for tubulin heterodimer compared to Z isomers. Finally, the compounds substituted by 2-, 3-, 4-nitro, 4-chloro-3- nitro, and 4-dimethylamine moieties on B ring were selected for synthesis step according to favorable docking results for tubulin heterodimer as main target (Table 1).*

Chemistry

A series of selected Aldimine-type Schiff base derivatives obtained from docking studies were synthesized following the reaction outlined in Scheme 1. The both methods (I and II in Scheme 1) were modified for the synthesis of compound **2** *but method II (fusion method) was applied for synthesis of recent compound because of the higher reaction yield (the yields of method I and II were 24% and 43% [31], respectively). The crude product was recrystallized from methanol to give compound* **2** *as precursor for Aldimine-type Schiff base derivatives. Thereafter, different aromatic aldehydes were added to compound* **2** *in the presence of few drops of HCl (Conc.) and absolute ethanol at 90–100 ℃ for 6–10 h, followed by immediately recrystallization from ethanol. The structures of these compounds were confirmed by FT-IR, ^{1}H NMR, ^{13}C NMR, and mass spectral data.*

Whereas the imine group (C=N) was reported as a photo-sensitive functional group. Most of imine-containing structures exhibited two isomerization manner; thermal isomerization (cis → trans) and photochemical isomerization (trans → cis) [32]. In the present study, all of compounds were synthesized in dark conditions and all of synthesis process (refluxed, work up, and recrystallization) were carried out in one day without elapsing time. Furthermore, the ^{1}H-NMR spectra of all synthesized compounds displayed one peak for –N=CH– (imine) (δ = 9.61–10.41 ppm). Meanwhile, the related calculated integrals indicated that almost one of the E or Z isomers was synthesized. In addition to E and Z isomeric states, these structures were able to tautomeric forms (thione and thiol). It must be noted that the FT-IR spectra of compounds almost displayed the both tautomeric forms (thione/thiol). However, the ^{1}H-NMR spectra displayed one peak for –NH/SH – (δ = 10.77–13.87 ppm).

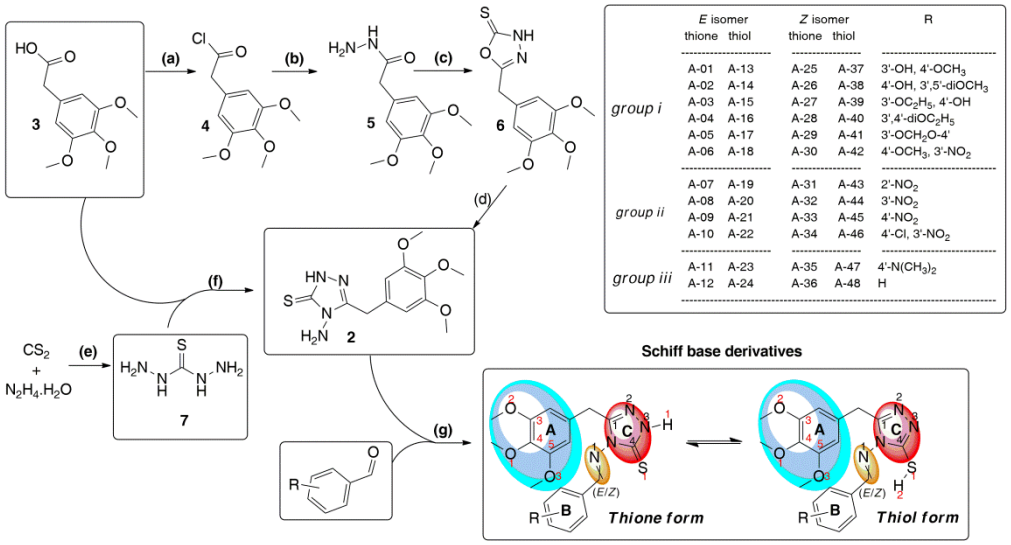

	E isomer thione	E isomer thiol	Z isomer thione	Z isomer thiol	R
group i	A-01	A-13	A-25	A-37	3'-OH, 4'-OCH_3
	A-02	A-14	A-26	A-38	4'-OH, 3',5'-diOCH_3
	A-03	A-15	A-27	A-39	3'-OC_2H_5, 4'-OH
	A-04	A-16	A-28	A-40	3',4'-diOC_2H_5
	A-05	A-17	A-29	A-41	3'-OCH_2O-4'
	A-06	A-18	A-30	A-42	4'-OCH_3, 3'-NO_2
group ii	A-07	A-19	A-31	A-43	2'-NO_2
	A-08	A-20	A-32	A-44	3'-NO_2
	A-09	A-21	A-33	A-45	4'-NO_2
	A-10	A-22	A-34	A-46	4'-Cl, 3'-NO_2
group iii	A-11	A-23	A-35	A-47	4'-$N(CH_3)_2$
	A-12	A-24	A-36	A-48	H

Scheme 1. *General reaction scheme for the synthesis of target compounds: Reagents and conditions: (I) Conventional method: (a) $SOCl_2$ refluxed 2 h, (b) N_2H_4, ethanol (abs.) refluxed 8 h, (c) KOH, CS_2, ethanol (abs.) refluxed 9 h, (d) N_2H_4, ethanol (abs.) refluxed 9 h; (II) Solvent free (fusion) method: (e) 1) dropwise, stirred at 0–5 °C, 2) refluxed 3 h, (f) fusion 140 °C and 170 °C for 6h in two steps, (g) ethanol (abs.), HCl (Conc.), refluxed for 6–10 h.*

There are several experimental methods for studying such isomerization including flash photolysis, NMR-, IR- and UV/Vis-spectroscopy. The same methods have been also applied for studying tautomeric transformations in solutions and in crystalline state [32, 33]. Recently, the quantum chemistry, the theoretical method, was applied for investigation of the stable forms of imine-containing compounds [32-34]. Therefore, we used geometry optimization for investigation of the stable forms of designed structures. So, compounds bearing 4-Nitro group on B ring (compounds **A-09**, **A-21**, **A-33**, *and* **A-45**) *were chosen as candidates for computational methods of quantum chemistry.*
As it can be seen the E isomers were more stable than Z isomers, and also the thione forms of two isomers were the most stable tautomer (Table 4).

Table 4. *Total energy (Hartree and KJmol^{-1}) values of the structures considered (B3LYP/6-31+G*) of 4-Nitro substituted Aldimine-type Schiff base*

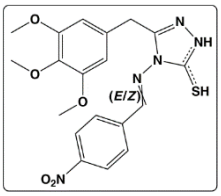

Isomeric form	Tautomeric form	Compound	Calculated energies	
			Hartree	kJmol^{-1}
E	*Thione*	*A-09*	*-1783.400719*	*-4682318.587577*
E	*Thiol*	*A-21*	*-1783.372632*	*-4682244.846445*
Z	*Thione*	*A-33*	*-1783.387754*	*-4682284.549387*
Z	*Thiol*	*A-45*	*-1783.362811*	*-4682219.059650*

Considering the higher stability of E isomers in quantum study and also the NMR results and synthesis conditions (that were described above), it seems that we synthesized and isolated the E isomers in synthesis steps.

Biological activity

a) Cytotoxicity assay: The potential cytotoxic effects of synthesized compounds against five cancer cell lines HT1080, HepG2, HT29, MCF-7, and A549 were evaluated by MTT assay. Doxorubicin, Colchicine, and Methotrexate were used as standard positive controls. The mean IC_{50} value of 4-Nitro substituted compound, Doxorubicin, Colchicine and Methotrexate against five mentioned cell lines was 11.84±1.01, 7.09±0.56, 3.83±0.20, and 0.40±0.03 µM, respectively. The compound 4-Nitro substituted compound (IC_{50} value of 5.28±0.72 µM) was more active than Doxorubicin (IC_{50} value of 6.12±0.47 µM) against HT29 cell line. The obtained pattern of mean IC_{50} values (4-Nitro> 2-Nitro> 4-Cl-3-Nitro>3-

*Nitro> 4-N(CH$_3$)$_2$ substituted compounds > compound (**2**) were approximately in agreement with the docking results on tubulin (**A-21** (4-Nitro) > **A-19** (2-Nitro) > **A-08** (3-Nitro) >**A-10** (4-Cl-3-nitro) > **A-11** (4-N(CH$_3$)$_2$> compound **2**) (Table 1 and Table 5). The comparison of the IC$_{50}$ values of compound **2** and Aldimine-type Schiff bases revealed the critical role of Schiff base pharmacophore for increasing the cytotoxic activity (Table 5). It must be noted that the position of the nitro group could also positively affected the cytotoxicity. For example, 4-nitro substituted compound inhibited the cell lines by mean IC$_{50}$ value of 11.84±1.01 µM while the 3-nitro substituted compound showed mean IC$_{50}$ value of 74.97±5.86 µM. In addition, the presence of 4-chloro moiety in compound **A-10** (4-Cl-3-Nitro) improved the inhibitory effect (approximately two fold) compared to 3-Nitro substituted compound (Table 5).*

Table 5. *In vitro cytotoxic activities (IC$_{50}$±S.E., µM) of the synthesized compounds and the standard controls.*

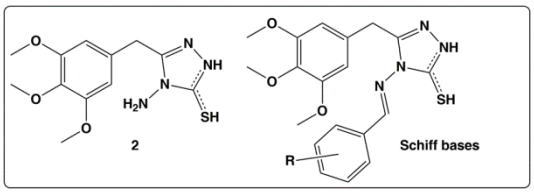

Compound	R	HT1080	HepG2	HT29	MCF-7	A549	Mean
2	-	*75.59±20.53*	*125.00±11.99*	*214.39±8.48*	*144.74±13.45*	*279.49±15.74*	*167.85±14.04*
A-07/19	*2-Nitro*	*17.98±0.32*	*24.21±1.70*	*19.82±1.87*	*25.36±2.59*	*12.25±0.30*	*19.92±1.36*
A-08/20	*3-Nitro*	*120.22±5.4*	*107.72±1.67*	*91.19±13.57*	*32.08±1.77*	*23.65±6.88*	*74.97±5.86*
A-09/21	*4-Nitro*	*13.74±0.48*	*17.21±0.43*	*5.28±0.72*	*9.67±1.36*	*13.32±2.07*	*11.84±1.01*
A-10/22	*4-Cl-3-Nitro*	*73.52±1.74*	*23.17±0.95*	*16.72±0.26*	*71.96±1.11*	*43.53±1.71*	*45.78±1.15*
A-11/23	*4-(CH$_3$)$_2$*	*117.02±9.64*	*26.22±1.79*	*41.81±1.18*	*74.58±2.09*	*79.89±4.89*	*67.90±3.92*
Doxorubicin	-	*12.69±1.23*	*6.74±0.48*	*6.12±0.47*	*3.51±0.32*	*6.40±0.31*	*7.09±0.56*
Colchicine	-	*3.76±0.31*	*5.10±0.27*	*3.35±0.05*	*4.08±0.31*	*2.87±0.06*	*3.83±0.20*
Methotrexate	-	*0.74±0.05*	*0.29±0.02*	*0.39±0.04*	*0.19±0.01*	*0.43±0.01*	*0.40±0.03*

The obtained results of the present study was in accordance to Banimustafa et al. who synthesized a series of 3-(trimethoxyphenyl)-2(3H)-thiazole thiones as combretastatin derivatives and evaluated their antiproliferative activity [35]. They found that the most potent agent inhibited the growth of T47D, MCF-7, and MDA-MB-231 cell lines by IC$_{50}$ of 16.3±3.7, 19.7±0.8, and 11.8±1.3 µgml^{-1}, respectively [35]. Among the combretastatin derivatives (1-aryl-6-(3,4,5-trimethoxyphenyl)-3(Z)-hexen-1,5-diynes) designed and synthesized in the study of Lo et al. the most effective compound was able to arrest the cell growth of A549, AGS (gastric cancer), and PC-3 (prostate cancer) by IC$_{50}$ value of 3.99, 0.13, and 0.51 µM, respectively [36]. Determination of the cytotoxic activity of a new series of 4 3,4-disubstituted-5-(3,4,5-trimethoxyphenyl)-4H-1,2,4-triazoles (as combretastatin analogs) revealed that the most active compound was able to inhibit HT-29, MCF-7, and HepG2 cell lines by the IC$_{50}$ values of 126.40, 63.72, and 31.72 µM, respectively [5].

b) Anti-tubulin assay: Following evaluation the cytotoxic effect of the synthesized derivatives, the ability of the most efficient compounds for inhibition of tubulin polymerization in vitro was demonstrated. As illustrated in Figure 3, 4-nitro substituted compound (was able to strongly inhibit tubulin polymerization and appeared to be even more potent than the reference compound Colchicine via elongation of tubulin polymerization procedure in the both applied concentrations of 5 µM and 15 µM. This compound elongated the tubulin assembly time compared to control (tubulin protein in the absence of any compound). The percent of tubulin polymerization inhibition in the case of 4-nitro substituted compound at two concentrations of 5 µM and 15 µM were found to be 78.2% and 81.5%, respectively, in comparison to control (Figure 3). Considering to the higher inhibition of tubulin assembly in the presence of 4-nitro substituted compound the IC$_{50}$ of this compound was determined and found to be 0.161±0.014 µM compared to that of Colchicine (0.189±0.012 µM). Although, 2-nitro substituted compound (30 µM) arrested the assembly of tubulin (inhibition percent of 59.7%) the inhibitory effect was found to be lower than Colchicine (5 µM, inhibition percent of 73.4%) (Figure 3). The positive effect of Paclitaxel (as a tubulin stabilizing agent) on polymerization of tubulin was also presented in Figure 3.

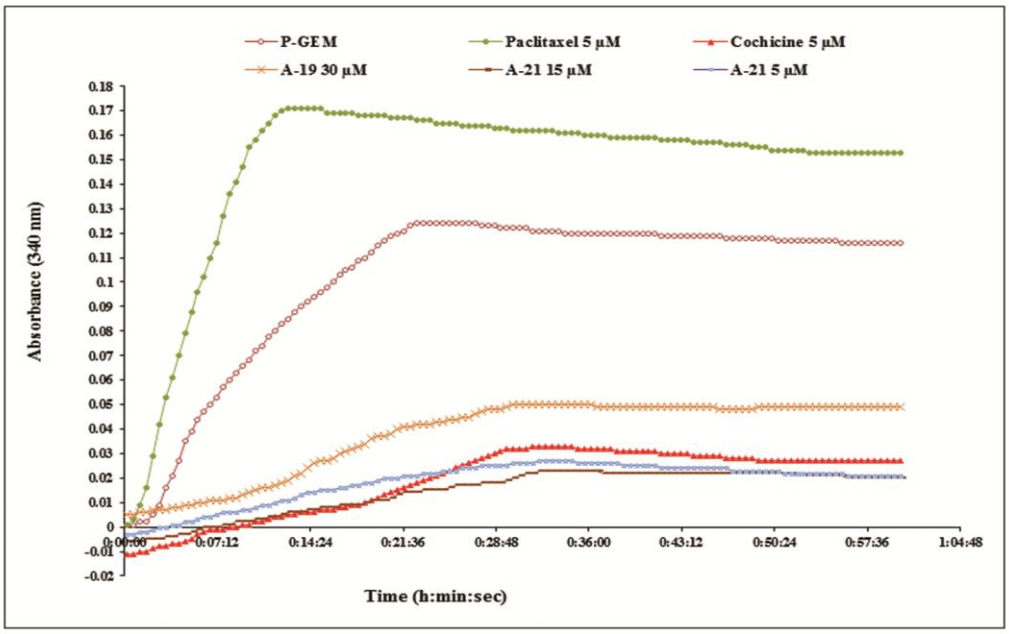

Figure 3. *Effects of 4-Nitro and 2-Nitro substituted compounds (***A-09/21** *and* **A-07/19**, *respectively) on tubulin polymerization. Each compound was added to tubulin solution (4 mgml*$^{-1}$*) prepared in P-GEM (general tubulin buffer containing 10.2% glycerol supplemented with 1 mM GTP) followed by monitoring of* A_{340} *using a Synergy 2 multi-mode plate reader during 60 min (intervals of 30 s) incubation at 37 °C.*

The obtained results of this section are in accordance with the molecular simulation studies which showed 4-nitro substituted compound (the best compound according to docking binding energy for tubulin) had hydrogen bonding interaction with Glnβ247 by SH group of 1,2,4-triazole-5-thiol ring and Glyα144 by nitro group while TMP moiety in A ring was well buried inside the hydrophobic pocket including Leuβ255, Lysβ254, and Alaβ250 in CBS (Figure 2c). On the other hand, 2-nitro substituted compound displayed two interaction models with CBS in αβ-tubulin heterodimers. The first model with energy binding of -9.07 kcalmol^{-1} *exhibited hydrogen bonding with Leuβ248, Alaβ250, and Glyα144 whereas TMP ring was placed near Leuβ248 and Lysβ254 in the hydrophobic pocket (Figure 2b). The second model with binding energy of -8.57 kcalmol*$^{-1}$ *showed hydrogen bonding between methoxy group in TMP ring and Cysβ241 together with oxygen atoms in nitro group exhibited hydrogen bonding with Vlaa181 and Lysβ352 (Figure 2a). This conformer was well buried in hydrophobic pocket and interacted by Leuβ255, Leuβ248, Metβ259, Alaβ317, and Alaβ316 (Figure 2a). It seems that these two compounds (4-nitro and 2-Nitro substituted compound) represented different models in CBS of αβ-tubulin heterodimer; i) H-bonding interaction with Cysβ241 [13] and ii) H-bonding contacts with Glyα144 [29, 30]. Furthermore, in the both models the hydrophobic interaction of TMP ring with critical hydrophobic residues of CBS in αβ-tubulin was observed.*

c) Antimicrobial assay: As represented in Table 6, which summarized the obtained results of antimicrobial activity of the synthesized compounds, 4-nitro substituted compound was the most active agent against all the three Gram-positive bacterial strains used in the present study by MIC[1] *value of less than 8 µgml*$^{-1}$*. 4-Nitro substituted compound was the second effective compound inhibited the growth of Gram-positive bacteria at concentration of 16 µgml*$^{-1}$*. Evaluation the antimicrobial effects of other three Aldimine-type Schiff bases (3-nitro, 4-Cl-3-nitro, and 4-N(*CH_3*)*$_2$ *substituted compounds) and* **2** *on Gram-positive bacterial strains revealed the MIC values of above 32 µgml*$^{-1}$ *among which compound* **2** *exhibited the lowest antibacterial activity against B. subtilis by MIC of 512 µgml*$^{-1}$*.*

The same pattern of efficacy (4-Nitro>2-Nitro>4-Cl-3-nitro>3-Nitro=4-N(CH_3*)*$_2$ *substituted compounds >* **2***) was attained after comparison of the results obtained from antibacterial activity of the tested compounds against Gram-negative bacteria (Table 6).*

In the case of yeast pathogens, C. neoformans was the most resistant strain which inhibited by 4-Nitro substituted compound at concentration of 32 µgml^{-1} *(Table 6). The observed MICs of 2-Nitro, 3-Nitro, 4-Cl-3-nitro, and 4-N(*CH_3*)*$_2$ *substituted compounds against C. neoformans were found to be 128 µgml*$^{-1}$*, 512 µgml*$^{-1}$*, 512 µgml*$^{-1}$*, and 512 µgml*$^{-1}$*, respectively (Table 6).*

[1] *The minimum inhibitory concentration*

Table 6. *The minimum inhibitory concentration (MIC, μgml^{-1}) of the synthesized compounds and the standard controls against the tested microorganisms.*

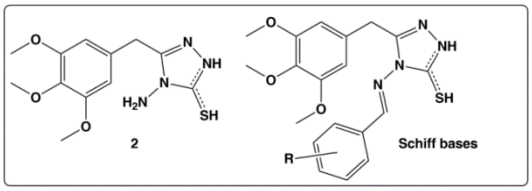

Compound	R	Gram-positive bacteria			Gram-negative bacteria				Yeast strains		
		1[a]	2[b]	3[c]	4[d]	5[e]	6[f]	7[g]	8[h]	9[i]	10[j]
2	-	256	512	256	1024	1024	512	1024	>1024	512	>1024
A-07/19	2-Nitro	16	16	16	32	16	<8	<8	16	32	128
08/20	3-Nitro	64	64	32	128	128	64	64	256	256	512
09/21	4-Nitro	<8	<8	<8	16	16	<8	<8	<8	<8	32
10/22	4-Cl-3-Nitro	32	64	32	64	64	32	64	64	64	512
11/23	4-$(CH_3)_2$	64	64	32	128	128	64	64	256	256	512
Ciprofloxacin	-	2	4	1.33	2.67	2	2	2	-	-	-
Fluconazole	-	-	-	-	-	-	-	-	8	8	16

[a] *Staphylococcus aureus (ATCC 29213);* [b] *Bacillus subtilis (ATCC 6051);* [c] *Micrococcus luteus (ATCC 4698);* [d] *Pseudomonas aeruginosa (ATCC 27853);* [e] *Klebsiella pneumoniae (ATCC 13883);* [f] *Escherichia coli (ATCC 25922);* [g] *Salmonella typhi (ATCC 6539);* [h] *Candida albicans (ATCC 10231);* [i] *Candida utilis (ATCC 9950);* [j] *Cryptococcus neoformans (ATCC 32045).*

The both applied standard antibacterial (Ciprofloxacin) and antifungal (Fluconazole) agents represented lower MICs compared to the tested compounds, except for 4-Nitro substituted compound which inhibited the growth of C. albicans and C. utilis at concentration below 8 μgml^{-1}. Huczyński, et al. evaluated the antibacterial effect of some colchicine derivatives against standard and clinically isolated and methicillin-resistant S. aureus and S. epidermidis. They reported an MIC range of 32–256 μgml^{-1} compared to those of Ciprofloxacin (0.125–64 μgml^{-1}) [37].

Conclusions

To sum up, forty eight new Aldimine-type Schiff base bearing 3,4,5-trimethoxyphenyl ring and 1,2,4-triazole-3-thiol/thione were designed and the best compounds according to the obtained results of the molecular docking study on tubulin complex (PDB code: 1SA0) were synthesized, and evaluated for cytotoxicity, anti-tubulin and antimicrobial activities. 4-Nitro substituted compound was introduced as the best compound in all applied biological assay and inhibited polymerization of tubulin at concentration of 5 μM. This compound represented higher anti-tubulin activity compared to Colchicine (IC_{50} values of 0.16±0.01 μM 0.19±0.01 μM, respectively).

Experimental

Molecular docking

The molecular docking simulations were executed using AutoDock 4.2 software [38] by Lamarckian Genetic Algorithm (LGA). The X-ray crystallographic structures of tubulin-colchicine: stathmin-like domain complex; human, S. aureus, and C. albicans DHFR; hsp90 and VEGFR2 were obtained from protein data bank (http://www.rcsb.org/) with PDB codes of 1SA0, 1PD8, 2W9S, 3QLS, 3MNR, and 3CJF, respectively and then the non-necessary moieties were deleted (ligands, non-important chains and co-enzymes and crystallographic waters except for hsp90). Structures of proteins were prepared using prepare PDB file for docking programs (http://swift.cmbi.ru.nl/servers/html). Other preprocessing steps were carried out by AutoDock Tools 1.5.6 (ADT) [39]. The Kollman charge was assigned for the proteins and non-polar hydrogens were merged. For ligands, structures were drawn using MarvinSketch 6.2.2 [40] and optimized by HyperChem software with semi-empirical PM3 method. Targets and ligands were prepared according to the tutorial of AutoDock Tools [39]. The grid maps of proteins were calculated by AutoGrid (a part of AutoDock software) [41]. The coordinates of center in grid box was superposed on root point on intrinsic ligands and then a grid box of 40×40×40 points in x, y, and z directions was built. All of the default parameters remained unchanged except for root mean square deviation (RMSD) tolerance of 1 Å and 250 docking runs measured for each ligand. The interactions of docked complex protein-ligand conformations were analyzed using AutoDock Tools 1.5.6 software [42]. Analyses for tubulin were performed according to clustering histogram of docking log file (.dlg) results of AutoDock. However, for other targets, results of clustering histogram was sorted based on the lowest energy of each compounds compared to ligands or standard inhibitors and only the first 22 cluster ranks were reported.

Chemistry

All chemicals were obtained from commercial suppliers of Merck Chemicals except for 3,4,5-trimethoxyphenyl acetic acid which provided by Alfa acer Co. (Karlsruhe, Germany). Melting points were identified with an Electrothermal 9200 capillary melting point apparatus. Bruker ALPHA FT-IR spectrometer was used for IR spectra (KBr discs). NMR (^{1}H and ^{13}C NMR) spectra in $CDCl_3$ and/or DMSO-d_6 solutions were taken on Bruker (400.13 MHz for ^{1}H and 100.61 MHz for ^{13}C at 25°C) spectrometers using TMS as internal standard. All chemical shift values were measured as δ (ppm). Splitting patterns are as follows: s, singlet; d, doublet; m, multiplet; b, broad; dd (doublet in doublet). Mass spectra were recorded on an Agilent technologies 5973 network mass selective detector (MSD) operating at an ionization potential of 70 eV. Elemental analyses were performed on an ECS 4010 CHNSO analyzer (Costech INC.). The purity of the compounds was evaluated by silica gel-coated aluminum sheets (Merck, Darmstadt, Germany) by thin-layer chromatography. The column chromatography was carried out using standard silica gel 60 (70-230 mesh) obtained from Merck chemicals. IUPAC names for all the novel compounds were given with the aid of MarvinSketch 6.2.2 [40].

*a) General procedure for the synthesis of 4-amino-3-[(3,4,5-trimethoxyphenyl)methyl]-4,5-dihydro-1H-1,2,4-triazole-5-thione (**Tn**), 4-amino-5-[(3,4,5-trimethoxyphenyl)methyl]-4H-1,2,4-triazole-3-thiol (**Tl**) (compound 2) (Scheme 1)*

*-Conventional method (I): The 3,4,5-trimethoxyphenyl acetic acid (**3**) (2.262 g, 10 mmol) was added to $SOCl_2$ (30 ml) and refluxed at 75 °C for 2 h in water bath followed by vacuum evaporating of the resulting solution to give compound **4**. Consequently, a solution of hydrazine hydrate 80% (12 ml) was added dropwise to compound **4** in absolute ethanol (30 ml) at 0–5 °C for 30 min and then refluxed at 85 °C for 8 h. The obtained mixture was evaporated in vacuum and the resulting semi-solid resin was purified using short column chromatography (n-hexane:ethyl acetate 70:30) to obtain compound **5**. A solution of potassium hydroxide (0.168 g, 3 mmol) in absolute ethanol (10 ml) was then added to a solution of **5** (0.481 g, 2 mmol) in absolute ethanol (40 ml) and stirred at 0–5 °C for 30 min followed by drop wise addition of carbon disulfide (1 ml) by a syringe for 30 min. The mixture was stirred at RT for 30 min and refluxed at 90 °C for 9 h. Subsequently, the suspension was concentrated by vacuum evaporation, acidified by HCl 4 N (pH 1–2), stirred for 1 h at 0–5 °C and kept overnight in freezer. Compound **6** was obtained after filtration, drying and purification by recrystallization from ethanol. Hydrazine hydrate 80% (17 ml) was then added dropwise into a solution of compound **6** (2.259 g, 8 mmol) in absolute ethanol (30 ml) at RT for 30 min and refluxed for 9 h. The resulting mixture was concentrated by vacuum evaporation and cold ethanol:water (30:70) solution was then added to give a solid, filtered and dried. The solid was recrystallized from methanol to give compound **2** as white crystals (Scheme 1). All synthesis and workup procedures were done away from the light.*

Milky white crystal; yield 24%; m.p. 171.8–173.6°C (methanol).

-Solvent free (fusion) method (II) [31]

1) General procedure for the synthesis of thiocarbazide (7)

*A solution of hydrazine hydrate 80% (30 ml) was stirred at 0–5 °C for 10 min and consequently, carbon disulfide (10 ml) was added dropwise over 30 min. The mixture was then stirred for 45 min and then refluxed at 75 °C for 3 h. Thereafter, the solution was cooled, and precipitated solids was filtered and dried. Compound **7** was purified by 4 times recrystallization from water and stored in the darkness (Scheme 1) [31].*

*2) General procedure for the synthesis of 4-amino-3-[(3,4,5-trimethoxyphenyl)methyl]-4,5-dihydro-1H-1,2,4-triazole-5-thione (**Tn**), 4-amino-5-[(3,4,5-trimethoxyphenyl)methyl]-4H-1,2,4-triazole-3-thiol (**Tl**) (**2**)*

*An equimolar mixture of compounds **3** (2.262 g, 10 mmol) and **7** (1.062 g, 10 mmol) was firstly heated and stirred on an oil bath at 130–140 °C for 5.5 h and then at 160–170 °C for 20 min. The boiling water was then added and stirred vigorously at RT for 30 min. The mixture was cooled and stirred at 5–10 °C for 1 h followed by filtering and drying. Compound **2** was then obtained by recrystallization from methanol. All synthesis procedures were conducted away from the light (Scheme 1) [31].*

Milky white crystal; yield 43%, m.p. 172.2–173.8 °C (methanol); FT-IR (KBr) υ_{max} (cm^{-1}): 3297.1, 3242.5 (N–H stretching), 3071.2, 3016.1 (Aromatic C–H stretching), 2926.7, 2835.1 (Aliphatic C–H stretching), 2749.6 (SH), 1606.1 (C=N), 1590.8 (C=C), 1332.2 (C–N), 1242.8, 1124.3 (C–O). ^{1}H NMR (400.13 MHz, $CDCl_3$) δ (ppm): 3.77 (s, 3 H, 4-OCH_3 in A ring), 3.79 (s, 6 H, 3-, 5-OCH_3 in A ring), 3.97 (s, 2 H, –CH_2–), 4.56 (s, 2 H, NH_2), 6.47 (s, 2 H, 2-, 6-H in A ring), 11.26 (s, 1 H, SH/NH tautomer in C ring). ^{13}C NMR (100.61 MHz, $CDCl_3$) δ (ppm): 31.43 (–CH_2–), 56.21 (3-, 5-OCH_3), 60.87 (4-OCH_3), 106.03 (C2, C6 in A ring), 129.64 (C1 in A ring), 137.35 (C4 in A ring), 152.02 (C1 in C ring, 153.47 (C3, C5 in A ring), 167.34 (C4 in C ring). EI-MS: m/z calcd. for $C_{12}H_{16}N_4O_3S$ $[M]^+$ 296.09; found 296.4 $[M]^+$(100.00), 297.4 $[M+1]^+$ (16.15), 298.4 $[M+2]^+$ (6.07), 280.4 $[M-NH_2]^+$ (56.79), 264.3 $[M-S]^+$ (4.67), 181.4 [(Trimethoxyphenyl-CH_2)$^+$] (8.83); Anal. calc. for $C_{12}H_{16}N_4O_3S$ (296.09): C 48.64, H 5.44, N 18.91, S 10.82; Found: C 48.51, H 5.25, N 18.59, S 11.09 .

b) General method for the preparation of aldimine-type Schiff bases

*Suitable aromatic aldehydes (10 mmol) and few drops of HCl Conc. were added to a mixture of compound **2** (2.964 g, 10 mmol) in absolute ethanol (60 ml). The mixture was then refluxed for 6–10 h with stirring, and consequently poured into crushed ice to give a solid which was*

filtered, washed with cold water, dried, and recrystallized from ethanol to give a series of Schiff bases. All above mentioned steps were performed away from the light (Scheme 1).

*E-4-{[(2-nitrophenyl)methylidene]amino}-3-[(3,4,5-trimethoxyphenyl)methyl]-4,5-dihydro-1H-1,2,4-triazole-5-thione (**A-07**), E-4-{[(2-nitrophenyl)methylidene]amino}-5-[(3,4,5-trimethoxyphenyl)methyl]-4H-1,2,4-triazole-3-thiol (**A-19**)*

Yellow powder; yield 65%; m.p. 198.6–200.6 ℃ (Ethanol); FT-IR (KBr) υ_{max} (cm^{-1}): 3257.87 (N–H stretching), 3090.24, 3015.40 (aromatic C–H stretching), 2969.26, 2925.76, 2902.39 (Aliphatic C–H stretching), 1593.92 (C=N), 1565.78 (C=C), 1536.07, 1345.79 (NO_2), 1335.99 (C–N), 1262.26 (C=S), 1244.99, 1121.25 (C–O). ^{1}H NMR (400.13 MHz, $CDCl_3$) δ (ppm): 3.70 (s, 6 H, 3-, 5-OCH_3 in A ring), 3.75 (s, 3 H, 4-OCH_3 in A ring), 4.03 (s, 2 H, –CH_2–), 6.43 (s, 2 H, 2-, 6-H in A ring), 7.61–7.71 (m, 2 H, 4'-, 5'-H in B ring), 7.93 (dd, J=7.58, 1.67 Hz, 1 H, 3'-H in B ring), 8.06 (dd, J=7.84, 1.41 Hz, 1 H, 6'-H in B ring), 10.41 (s, 1 H, –N=CH–), 11.03 (s, 1 H, SH/NH tautomer in C ring). ^{13}C NMR (100.61 MHz, DMSO-d_6) δ (ppm): 31.27 (–CH_2–), 56.15 (3-, 5-OCH_3), 60.40 (4-OCH_3), 106.78 (C2,C6 in A ring), 125.37 (C3' in B ring), 127.39 (C1 in A ring), 129.46 (C6' in B ring), 131.01 (C1' in B ring), 133.39 (C5' in B ring), 134.41 (C4' in B ring), 136.87 (C4 in A ring), 149.17 (C2' in B ring), 151.30 (C1'' in C ring), 153.28 (C3, C5 in A ring), 155.94 (–N=CH–), 162.04 (C4'' in C ring). EI-MS: m/z calcd. for $C_{19}H_{19}N_5O_5S$ $[M]^+$ 429.11; found 429.5$[M]^+$ (5.41),430.6 $[M+1]^+$ (1.84), 431.4 $[M+2]^+$ (0.57), 383.5 $[M-NO_2]^+$ (2.34), 281.4 [3-(3,4,5-trimethoxybenzyl)-1H-1,2,4-triazole-5(4H)-thione]$^+$ (27.72), 230.3 [(4-((2-nitrobenzylidene)amino)-4H-1,2,4-triazol-3-yl)methylium]$^+$ (49.92), 103.3 [Benzonitrile]$^+$ (100.00). Anal. calc. for $C_{19}H_{19}N_5O_5S$ (429.11): C 53.14, H 4.46, N 16.31, S 7.47; Found: C 53.46, H 4.33, N 16.54, S 7.19.

*E-4-{[(3-nitrophenyl)methylidene]amino}-3-[(3,4,5-trimethoxyphenyl)methyl]-4,5-dihydro-1H-1,2,4-triazole-5-thione (**A-08**), E-4-{[(3-nitrophenyl)methylidene]amino}-5-[(3,4,5-trimethoxyphenyl)methyl]-4H-1,2,4-triazole-3-thiol (**A-20**)*

Pale yellow powder; yield 79%; m.p. 214.5–216 ℃ (Ethanol); FT-IR (KBr) υ_{max} (cm^{-1}): 3104.87, 3057.59 (aromatic C–H stretching), 2944.15, 2838.93 (aliphatic C–H stretching), 2787.54 (S–H), 1587.63 (C=N), 1535.29, 1350.81 (NO_2), 1335.03 (C–N), 1289.31 (C=S), 1249.14, 1122.18 (C–O). ^{1}H NMR (400.13 MHz, $CDCl_3$) δ (ppm): 3.71 (s, 6 H, 3-, 5-OCH_3 in A ring), 3.73 (s, 3 H, 4-OCH_3 in A ring), 4.09 (s, 2 H, –CH_2–), 6.47 (s, 2 H, 2-, 6-H in A ring), 7.62 (t, J=7.96 Hz, 1 H, 5'-H in B ring), 8.03 (dt, J=7.71, 1.28 Hz,1 H, 6'-H in B ring), 8.31 (ddd, J=8.22, 2.31, 1.03 Hz, 1 H, 4'-H in B ring), 8.69 (t, J=1.93 Hz, 1 H, 2'-H in B ring), 10.15 (br. s., 1 H, –N=CH–), 10.77 (s, 1 H, SH/NH tautomer in C ring). ^{13}C NMR (100.61 MHz, DMSO-d_6) δ (ppm): 31.38 (–CH_2–), 56.13 (3-, 5-OCH_3 in A ring), 60.38 (4-OCH_3 in A ring), 106.70 (C2,C6 in A ring), 123.05 (C4' in B ring), 127.23 (C2' in B ring), 131.03 (C1 in A ring), 131.34 (C5' in B ring), 134.41 (C1' in B ring), 135.03 (C6' in B ring), 136.85 (C4 in A ring), 148.80 (C3' in B ring), 150.93 (C1'' in C ring), 153.30 (C3, C5 in A ring), 160.76 (–N=CH–), 162.02 (C4'' in C ring). EI-MS (%): m/z calcd. for $C_{19}H_{19}N_5O_5S$ $[M]^+$ 429.11; found 429.4 $[M]^+$(29.9),430.5 $[M+1]^+$ (7.11), 431.4 $[M+2]^+$ (2.49), 352.4 [M-NO_2 and S]$^+$ (3.00), 281.4 [3-(3,4,5-trimethoxybenzyl)-1H-1,2,4-triazole-5(4H)-thione]$^+$ (59.00), 103.3 [Benzonitrile]$^+$ (48.05), 91.3 [Cyclohepta-2,4,6-trien-1-ylium] (100.00). Anal. calc. for $C_{19}H_{19}N_5O_5S$ (429.11): C 53.14, H 4.46, N 16.31, S 7.47; Found: C 53.42, H 4.07, N 16.54, S 7.18.

*E-4-{[(4-nitrophenyl)methylidene]amino}-3-[(3,4,5-trimethoxyphenyl)methyl]-4,5-dihydro-1H-1,2,4-triazole-5-thione (**A-09**), E-4-{[(4-nitrophenyl)methylidene]amino}-5-[(3,4,5-trimethoxyphenyl)methyl]-4H-1,2,4-triazole-3-thiol (**A-21**)*

Yellow powder; yield 85%; m.p. 240.3–240.8 ℃ (ethanol); FT-IR (KBr) υ_{max} (cm^{-1}): 3104.71, 3062.59 (aromatic C–H stretching), 2950.04, 2840.98 (aliphatic C–H stretching), 2777.92 (SH), 1596.30 (C=N), 1579.03 (C=C), 1521.43, 1342.27 (NO_2), 1316.41 (C–N), 1283.64 (C=S), 1253.52, 1125.52 (C–O). ^{1}H NMR (400.13 MHz, $CDCl_3$) δ (ppm): 3.72 (s, 6 H, 3-, 5-OCH_3 in A ring), 3.75 (s, 3 H, 4- OCH_3 in A ring), 4.09 (s, 2 H, –CH_2–), 6.46 (s, 2 H, 2-, 6-H in A ring), 7.97 (d, J=8.73 Hz, 2 H, 2'-, 6'-H in B ring), 8.29 (d, J=8.73 Hz, 2 H, 3'-, 5'-H in B ring), 9.83 (br. s., 1 H, –N=CH–), 10.83 (s, 1 H, SH/NH tautomer in C ring). ^{13}C NMR (100.61 MHz, $CDCl_3$ + DMSO-d_6) δ (ppm): 36.27 (–CH_2–), 60.76 (3-, 5-OCH_3), 65.26 (4-OCH_3), 110.92 (C2,C6 in A ring), 128.88 (C3', C5' in B ring), 134.07 (C2', C6' in B ring), 135.27 (C1 in A ring), 143.74 (C4 in A ring), 153.27 (C1' in B ring), 154.39 (C4' in B ring), 155.65 (C3, C5 in A ring), 157.93 (–N=CH–), 160.86 (C1'' in C ring), 166.94 (C4'' in C ring). EI-MS (%): m/z calcd. for $C_{19}H_{19}N_5O_5S$ $[M]^+$ 429.11; found 429.4 $[M]^+$(35.35),430.4 $[M+1]^+$ (9.42), 431.4 $[M+2]^+$ (2.42), 296.3 [4-Amino-3-(3,4,5-trimethoxybenzyl)-1H-1,2,4-triazole-5(4H)-thione]$^+$ (52.47), 281.3 [3-(3,4,5-trimethoxybenzyl)-1H-1,2,4-triazole-5(4H)-thione]$^+$ (100.00). Anal. calc. for $C_{19}H_{19}N_5O_5S$ (429.11): C 53.14, H 4.46, N 16.31, S 7.47; found: C 53.27, H 4.19, N 16.51, S 7.09.

*E-4-{[(4-chloro-3-nitrophenyl)methylidene]amino}-3-[(3,4,5-trimethoxyphenyl)methyl]-4,5-dihydro-1H-1,2,4-triazole-5-thione (**A-10**), E-4-{[(4-chloro-3-nitrophenyl)methylidene]amino}-5-[(3,4,5-trimethoxyphenyl)methyl]-4H-1,2,4-triazole-3-thiol (**A-22**)*

Pale yellow solid; yield 79%; m.p. 243.3–244 ℃ (ethanol); FT-IR (KBr) υ_{max} (cm^{-1}): 3099.79, 3060.86 (aromatic C–H stretching), 2994.57, 2947.26, 2833.93 (aliphatic C–H stretching), 2779.42 (SH), 1597.83 (C=N), 1583.16 (C=C), 1537.31, 1359.18 (NO_2), 1334.65 (C-N); 1281.56 (C=S), 1254.98, 1128.35 (C-O), 758.85 (C-Cl). ^{1}H NMR (400.13 MHz, DMSO-d_6) δ (ppm): 3.50 (s, 3 H, 4-OCH_3 in A ring), 3.57 (s, 6 H, 3-, 5-OCH_3 in A ring), , 4.04(s, 2 H, –CH_2–), 6.53 (s, 2 H, 2-, 6-H in A ring), 7.88 (d, J=8.22 Hz, 1 H, 6'-H in B ring), 8.13 (dd, J=8.48, 2.06 Hz, 1 H, 5'-H in B ring), 8.55 (d, J=1.80 Hz, 1 H, 2'-H in B ring), 10.24 (s, 1 H, –N=CH–), 13.87 (s, 1 H, SH/NH tautomer in C ring). ^{13}C NMR (100.61 MHz, DMSO-d_6) δ (ppm): 31.23 (–CH_2–), 56.16 (3-, 5-OCH_3), 60.39 (4-OCH_3), 106.74 (C2,C6 in A ring), 124.99 (C2' in B ring), 128.74 (C1 in A ring), 131.06 (C5' in B ring), 133.01 (C6' in B ring), 133.33 (C4' in B ring), 133.58 (C1' in B ring), 136.84 (C4 in A ring), 148.72 (C3' in B ring), 151.14 (C1'' in C ring), 153.28 (C3, C5 in A ring), 158.56 (–N=CH–), 162.01 (C4'' in C ring). EI-MS (%): m/z calcd. for $C_{19}H_{18}ClN_5O_5S$ $[M]^+$ 463.07; found 463.4 $[M]^+$(35.39),464.4 $[M+1]^+$ (8.51), 465.4 $[M+2]^+$ (13.42), 466.4 $[M+3]^+$ (3.43), 467.4 $[M+4]^+$ (1.01), 429.5 $[M-Cl]^+$ (2.17), 296.4 [4-amino-3-(3,4,5-trimethoxybenzyl)-1H-1,2,4-triazole-5(4H)-

thione]$^+$ (16.01), 281.4 [3-(3,4,5-trimethoxybenzyl)-1H-1,2,4-triazole-5(4H)-thione]$^+$ (100.00), 266.3 [4-(3,4,5-trimethoxybenzyl)-1,2-diazete-3-thiol]$^+$ (96.03). Anal. calc. for $C_{19}H_{18}ClN_5O_5S$ (463.07): C 49.19, H 3.91, N 15.10, S 6.91; Found: C 49.45, H 3.78, N 15.32, S 6.52.

*E-4-({[4-(dimethylamino)phenyl]methylidene}amino)-3-[(3,4,5-trimethoxyphenyl)methyl]-4,5-dihydro-1H-1,2,4-triazole-5-thione (**A-11**), E-4-({[4-(dimethylamino)phenyl]methylidene}amino)-5-[(3,4,5-trimethoxyphenyl)methyl]-4H-1,2,4-triazole-3-thiol (**A-23**)*

Pale yellow crystal; 62%; m.p. 160–162°C (ethanol); FT-IR (KBr) υ_{max} (cm^{-1}): 3289.87 (N–H stretching) 3112.56, 3043.07 (aromatic C–H stretching), 2922.49, 2933.76 (aliphatic C–H stretching), 1613.47 (C=N), 1586.56 (C=C), 1371.18 (C–N); 1300.50 (C=S), 1244.21, 1132.56 (C–O). ^{1}H NMR (400.13 MHz, $CDCl_3$) δ (ppm): 3.10 (s, 6 H, 4-N(CH_3)$_2$ in B ring), 3.73 (s, 6 H, 3-, 5-OCH_3 in A ring), 3.80 (s, 3 H, 4-OCH_3 in A ring), 4.08 (s, 2 H, –CH_2–), 6.55 (s, 2 H, 2-, 6-H in A ring), 6.74 (d, J=8.99 Hz, 2 H, 3'-, 5'-H in B ring), 7.75 (d, J=8.99 Hz, 2 H, 2'-, 6'-H in B ring), 9.61 (br. s., 1 H, –N=CH–), 11.43 (br. s., 1 H, SH/NH tautomer in C ring). ^{13}C NMR (100.61 MHz, $CDCl_3$) δ (ppm): 31.80 (–CH_2–), 40.16 (4-N(CH_3)$_2$ in B ring), 55.96 (3-, 5-OCH_3), 60.81 (4-OCH_3), 106.14 (C2,C6 in A ring), 111.55 (C3', C5' in B ring), 119.40 (C1' in B ring), 130.31 (C1 in A ring), 130.68 (C2', C6' in B ring), 136.97 (C4 in A ring), 151.15 (C1'' in C ring), 153.21 (C3, C5 in A ring), 153.31 (C4' in B ring), 161.97 (C4'' in C ring), 164.06 (–N=CH–). EI-MS (%): m/z calcd. for $C_{21}H_{25}N_5O_3S$ [M]$^+$ 427.17 found 427.5 [M]$^+$ (8.53),428.5 [M+1]$^+$ (1.99), 429.5 [M+2]$^+$ (0.69), 381.5 [M- CH_3 and S]$^+$ (2.10), 352.4[M-N(CH_3)$_2$ and S]$^+$ (3.42), 296.4 [4-Amino-3-(3,4,5-trimethoxybenzyl)-1H-1,2,4-triazole-5(4H)-thione]$^+$ (3.67), 281.4 [3-(3,4,5-trimethoxybenzyl)-1H-1,2,4-triazole-5(4H)-thione]$^+$ (18.29), 146.3 [4-(dimethylamino)benzonitrile]$^+$ (59.59), 103.3 [benzonitrile]$^+$ (42.77), 91.3 [Cyclohepta-2,4,6-trien-1-ylium]$^+$ (100.00). Anal. calc. for $C_{21}H_{25}N_5O_3S$ (427.17): C 59.00, H 5.89, N 16.38, S 7.50, Found: C 58.79, H 5.78, N 16.77, S 6.99.

Geometry optimization method

All calculations were performed by Gaussian 98W software [43]. The geometry optimizations of all four compounds were carried out at the B3LYP density functional study by using basis set of 6-31+G. The calculated energies of all compounds in hartree and $kJmol^{-1}$ units are displayed in Table 4.*

Biological activity

a) Cytotoxicity assay: The MTT based cytotoxicity assay was used for evaluation of the inhibitory activity of the synthesized compounds. The applied cell lines (A549, HT1080, HT29, HepG2, and MCF-7) were purchased from Iranian Biological Resource Center (IBRC) Tehran, Iran and sub-cultured in DMEM medium containing 10% FBS and antibiotics including penicillin (100 $unitsml^{-1}$) and streptomycin (100 μgml^{-1}) at 37 °C in a CO_2 incubator (5% CO_2). The attached cells were then removed at logarithmic phase of growth and 15000 cells was consequently transferred to each well of flat bottom 96-well microplate followed by incubation at 37 °C for 24 h. The attached cells were then exposed by the tested compounds (final concentration range of 0.195–300 μM), Doxorubicin (final concentration range of 0.500–16 μM), Colchicine (final concentration range of 0.016–16 μM), and Methotrexate (final concentration range of 0.031–8 μM) (all as positive controls) and incubated for further 24 h. The culture media of the treated sample was subsequently replaced by 20 μl DMEM medium containing MTT (5 $mgml^{-1}$) and incubated for an additional 4 h followed by dissolving the produced formazan crystal using DMSO (100 μl) and measuring the related absorbance at 570 nm. All mentioned procedures were repeated three times and the obtained results were applied for determination of IC_{50}.

b) Tubulin inhibitory studies: Tubulin polymerization assay was determined by monitoring the change in turbidity (A_{340nm}) according to the protocol described by supplier (Cytoskeleton, Denver, CO, USA). In brief, into the desired well of a half volume 96-well microplate 10 μl of 10X concentration of the selected compound and 100 μl of ice cold tubulin solution [prepared by re-suspending of the purified lyophilized porcine brain tubulin in glycerol containing G-PEM buffer (80 mM PIPES pH 6.9, 1 mM EGTA, 0.5 mM $MgCl_2$, 1 mM GTP, and 10.2% (v/v) glycerol)] were added and the related optical density at 340 nm was monitored by a Synergy 2 multi-mode plate reader (Biotek, Winooski, VT, USA) during 60 min (intervals of 30 s) incubation at 37 °C. In addition, tubulin polymerization inhibition percent (TPI%) was calculated using the following equation:

$$TPI\% = \left[1 - \left(\frac{\mathrm{MaxAT}}{\mathrm{MaxAC}}\right)\right] \times 100$$

Where MaxAT and MaxAC were regarded as maximum absorbance of the test and control, respectively. In the case of colchicine and the most potent compound the IC_{50} was also evaluated after measuring the TPI% in the presence of different concentrations of each compound.

c) Microplate-based antimicrobial activity determination: To estimate the antimicrobial effect of the prepared compounds a modified method of Ahmed et al. [44] and Aumeeruddy-Elalfi et al. [45] was conducted as follow. Firstly, a serial dilution of each synthesized compound (8–1024 μgml^{-1}) was prepared in 96-well round-bottle microplate and the freshly prepared inoculum of each tested microbial pathogen (Staphylococcus aureus, ATCC 29213; Bacillus subtilis, ATCC 6051; Micrococcus luteus, ATCC 4698; Pseudomonas aeruginosa, ATCC 27853; Klebsiella pneumoniae, ATCC 13883; Escherichia coli, ATCC 25922; Salmonella typhi, ATCC 6539;Candida albicans, ATCC 10231;Candida utilis, ATCC 9950; and Cryptococcus neoformans, ATCC 32045) was added to the desired well to reach final concentration of 10^4 $CFUml^{-1}$. After incubation of the microplates at 37 °C for appropriate time (24 h for bacterial strains, 48 h for Candida species and 72 h for C. neoformans) an amount of 40 μl of the tetrazolium salt (2-(4-iodophenyl)-3-(4-nitrophenyl)-5-phenyl tetrazolium chloride, INT, 0.6 $mgml^{-1}$) was added to each well and their absorbance was measured at 490 nm after 20 min incubation at 37 °C. The MICs was then determined based on the lowest

concentration in which no absorbance at 490 nm was detected. In a similar trial, un-inoculated media and inoculated media inserted by each microbial strain was applied as negative and positive control, respectively. The antifungal drug Fluconazole (final concentration range of 1–16 μgml^{-1}) and antibacterial agent Ciprofloxacin (concentration range of 0.5–8 μgml^{-1}) were applied as standard control. Three independent replicate of each experiment was conducted and mean of the obtained results were reported.

Supplementary Material

Supporting information for this article is available on the WWW under http://dx.doi.org/10.1002/MS-number.

Acknowledgements

This work was supported by Isfahan University of Medical Sciences, Isfahan, Iran [grant number 190068]. The authors would like to appreciate Prof. Mohammad Ali Faramarzi for his kindly consultations.

Author Contribution Statement

Project was designed by G. Khodarahmi, A. Ameri, F. Hassanzadeh, and G. Hakimelahi. Molecular docking studies and analysis of results were performed by A. Ameri. Experiments, data analysis, and writing of the manuscript were carried out by A. Ameri and G. Khodarahmi. Cytotoxicity, antimicrobial, and Tubulin polymerization assays and interpretation of results were performed by A. Ameri and H. Forootanfar.

References

[1] *A. Assadieskandar, M. Amini, S. N. Ostad, G. H. Riazi, T. Cheraghi-Shavi, B. Shafiei, A. Shafiee, 'Design, synthesis, cytotoxic evaluation and tubulin inhibitory activity of 4-aryl-5-(3,4,5-trimethoxyphenyl)-2-alkylthio-1H-imidazole derivatives', Bioorg. Med. Chem.* **2013**, *21, 2703–2709.*

[2] *N. M. O'Boyle, M. Carr, L. M. Greene, N. O. Keely, A. J. S. Knox, T. McCabe, D. G. Lloyd, D. M. Zisterer, M. J. Meegan, 'Synthesis, biochemical and molecular modelling studies of antiproliferative azetidinones causing microtubule disruption and mitotic catastrophe', Eur. J. Med. Chem.* **2011**, *46, 4595–4607.*

[3] *R. Romagnoli, P. G. Baraldi, M. K. Salvador, F. Prencipe, C. Lopez-Cara, S. Schiaffino Ortega, A. Brancale, E. Hamel, I. Castagliuolo, S. Mitola, R. Ronca , R. Bortolozzi , E. Porcù, G. Basso, G. Viola, 'Design, synthesis, in vitro, and in vivo anticancer and antiangiogenic activity of novel 3-arylaminobenzofuran derivatives targeting the colchicine site on tubulin', J. Med. Chem.* **2015**, *58, 3209–3222.*

[4] *R. Romagnoli, P. G. Baraldi, M. K. Salvador, M. E. Camacho, D. Preti, M. A. Tabrizi, M. Bassetto, A. Brancale, E. Hamel, R. Bortolozzi, G. Basso, G. Viola, 'Synthesis and biological evaluation of 2-substituted-4-(3',4',5'-trimethoxyphenyl)-5-aryl thiazoles as anticancer agents', Bioorg. Med. Chem.* **2012**, *20, 7083–7094.*

[5] *P. L. Zhao, A. N. Duan, M. Zou, H. K. Yang, W. W. You, S. G. Wu, 'Synthesis and cytotoxicity of 3,4-disubstituted-5-(3,4,5-trimethoxyphenyl)-4H-1,2,4-triazoles and novel 5,6-dihydro-[1,2,4]triazolo[3,4-b][1,3,4]thiadiazole derivatives bearing 3,4,5-trimethoxyphenyl moiety', Bioorg. Med. Chem. Lett.* **2012**, *22, 4471–4474.*

[6] *Y. Hu, X. Lu, C. K., Y. Luo, R. Yan, Q. S. Li, H. L. Zhu, 'Design, synthesis, biological evaluation and molecular modeling of 1,3,4-oxadiazoline analogs of combretastatin-A4 as novel antitubulin agents', Bioorg. Med. Chem.* **2012**, *20, 903–909.*

[7] *A. S. Negi, Y. Gautam, S. Alam, D. Chanda, S. Luqman, J. Sarkar, F. Khan, R. Konwar, 'Natural antitubulin agents: Importance of 3,4,5-trimethoxyphenyl fragment', Bioorg. Med. Chem.* **2015**, *23, 373–389.*

[8] *Z. Wen, J. Xu, Z. Wang, H. Qi, Q. Xu, Z. Bai, Q. Zhang, K. Bao, Y. Wu, W. Zhang, '3-(3,4,5-Trimethoxyphenylselenyl)-1H-indoles and their selenoxides as combretastatin A-4 analogs: Microwave-assisted synthesis and biological evaluation', Eur. J. Med. Chem.* **2015**, *90, 184–194.*

[9] *R. Romagnoli, P. G. Baraldi, O. Cruz-Lopez, M. Tolomeo, A. D. Cristina, R. M. Pipitone, S. Grimaudo, J. Balzarini, A. Brancale, E. Hamel, 'Synthesis of novel antimitotic agents based on 2-amino-3-aroyl-5-(hetero) arylethynyl thiophene derivatives', Bioorg. Med. Chem. Lett.* **2011**, *21, 2746–2751.*

[10] *A. Chaudhary, P. Sharma, G. Bhardwaj, V. Jain, P. Bharatam, B. Shrivastav, R. Roy, 'Synthesis, biological evaluation, and molecular modeling studies of novel heterocyclic compounds as anti-proliferative agents', Med. Chem. Res.* **2013**, *22, 5654–5669.*

[11] *R. B. G. Ravelli, B. Gigant, P. A. Curmi, I. Jourdain, S. Lachkar, A. Sobel, M. Knossow, 'Insight into tubulin regulation from a complex with colchicine and a stathmin-like domain', Nature* **2004**, *428, 198–202.*

[12] M. Botta, S. Forli, M. Magnani, F. Manetti, in Tubulin-Binding Agents, Vol. 286 (Ed.: T. Carlomagno), Springer, Berlin Heidelberg, 2009, p. 279–328.

[13] M. M. Niu, J. Y. Qin, C. P. Tian, X. F. Yan, F. G. Dong, Z. Q. Cheng, G. Fida, M. Yang, H. Chen, Y. Q. Gu, 'Tubulin inhibitors: pharmacophore modeling, virtual screening and molecular docking', Acta. Pharmacol. Sin. **2014**, 35, 967–979.

[14] T. L. Nguyen, C. McGrath, A. R. Hermone, J. C. Burnett, D. W. Zaharevitz, B. W. Day, P. Wipf, E. Hamel, R. Gussio, 'A common pharmacophore for a diverse set of colchicine site inhibitors using a structure-based approach', J. Med. Chem. **2005**, 48, 6107–6116.

[15] O. Zefirova, A. Diikov, N. Zyk, N. Zefirov, 'Ligands of the colchicine site of tubulin: a common pharmacophore and new structural classes', Russ. Chem. Bull. **2007**, 56, 680–688.

[16] C. Da, S. L. Mooberry, J. T. Gupton, G. E. Kellogg, 'How to deal with low-resolution target structures: Using SAR, ensemble docking, hydropathic analysis, and 3D-QSAR to definitively map the αβ-tubulin colchicine site', J. Med. Chem. **2013**, 56, 7382–7395.

[17] C.-H. Jeong, H. B. Park, W. J. Jang, S. H. Jung, Y. H. Seo, 'Discovery of hybrid Hsp90 inhibitors and their anti-neoplastic effects against gefitinib-resistant non-small cell lung cancer (NSCLC)', Bioorg. Med. Chem. Lett. **2014**, 24, 224–227.

[18] A. Gangjee, O. A. Namjoshi, S. Raghavan, S. F. Queener, R. L. Kisliuk, V. Cody, 'Design, synthesis, and molecular modeling of novel pyrido [2, 3-d] pyrimidine analogues as antifolates; application of Buchwald–Hartwig aminations of heterocycles', J. Med. Chem. **2013**, 56, 4422–4441.

[19] A. Saeed, A. Mumtaz, 'Novel isochroman-triazoles and thiadiazole hybrids: design, synthesis and antimicrobial activity', J. Saudi. Chem. Soc. **2017**, 21, 186–192.

[20] D. Sriram, T. Ratan Bal, P. Yogeeswari, 'Aminopyrimidinimino isatin analogues: Design of novel nonnucleoside HIV-1 reverse transcriptase inhibitors with broadspectrum chemotherapeutic properties', J. Pharm. Pharm. Sci. **2005**, 8, 565–577.

[21] H. Hussain, A. Al-Harrasi, A. Al-Rawahi, I. R. Green, S. Gibbons, 'Fruitful decade for antileishmanial compounds from 2002 to late 2011', Chem. Rev. **2014**, 114, 10369–10428.

[22] M. M. Kamel, N. Y. M. Abdo, 'Synthesis of novel 1,2,4-triazoles, triazolothiadiazines and triazolothiadiazoles as potential anticancer agents', Eur. J. Med. Chem. **2014**, 86, 75–80.

[23] L. Y. Zhang, B. L. Wang, Y. Z. Zhan, Y. Zhang, X. Zhang, Z. M. Li, 'Synthesis and biological activities of some fluorine-and piperazine-containing 1,2,4-triazole thione derivatives', Chin. Chem. Lett. **2016**, 27, 163–167.

[24] M. Koparir, C. Orek, P. Koparir, K. Sarac, 'Synthesis, experimental, theoretical characterization and biological activities of 4-ethyl-5-(2-hydroxyphenyl)-2H-1,2,4-triazole-3 (4H)-thione', Spectrochim. Acta A Mol. Biomol. Spectrosc. **2013**, 105, 522–531.

[25] K. Sztanke, T. Tuzimski, J. Rzymowska, K. Pasternak, M. Kandefer-Szerszeń, 'Synthesis, determination of the lipophilicity, anticancer and antimicrobial properties of some fused 1,2,4-triazole derivatives', Eur. J. Med. Chem. **2008**, 43, 404–419.

[26] Z. Li, Z. Gu, K. Yin, R. Zhang, Q. Deng, J. Xiang, 'Synthesis of substituted-phenyl-1,2,4-triazol-3-thione analogues with modified d-glucopyranosyl residues and their antiproliferative activities', Eur. J. Med. Chem. **2009**, 44, 4716–4720.

[27] K. Sztanke, A. Maziarka, A. Osinka, M. Sztanke, 'An insight into synthetic Schiff bases revealing antiproliferative activities in vitro', Bioorg. Med. Chem. **2013**, 21, 3648–3666.

[28] A. Ganguly, P. Chakraborty, K. Banerjee, S. K. Choudhuri, 'The role of a Schiff base scaffold, N-(2-hydroxy acetophenone) glycinate-in overcoming multidrug resistance in cancer', Eur. J. Pharm. Sci. **2014**, 51, 96–109.

[29] N. Kandakatla, G. Ramakrishnan, J. Karthikeyan, R. Chekkara, 'Pharmacophore modeling, atom based 3D-QSAR and docking studies of chalcone derivatives as tubulin inhibitors', Orient. J. Chem. **2014**, 30, 1083–1098.

[30] T. T. Zhao, X. Lu, X. H. Yang, L. M. Wang, X. Li, Z. C. Wang, H. B. Gong, H. L. Zhu, 'Synthesis, biological evaluation, and molecular docking studies of 2,6-dinitro-4-(trifluoromethyl)phenoxysalicylaldoxime derivatives as novel antitubulin agents', Bioorg. Med. Chem. **2012**, 20, 3233–3241.

[31] A. Ameri, G. Khodarahmi, F. Hassanzadeh, H. Forootanfar, G. H. Hakimelahi, 'Novel Aldimine-Type Schiff Bases of 4-Amino-5-[(3, 4, 5-trimethoxyphenyl) methyl]-1, 2, 4-triazole-3-thione/thiol: Docking Study, Synthesis, Biological Evaluation, and Anti-Tubulin Activity', Arch. Pharm. Chem. Life Sci. **2016**, 349, 662–681.

[32] Y. Luo, M. Utecht, J. Dokić, S. Korchak, H.M. Vieth, R. Haag, P. Saalfrank, 'Cis–trans isomerisation of substituted aromatic imines: a comparative experimental and theoretical study', Chem. Phys. Chem. **2011**, 12, 2311–2321.

[33] M. D. Davari, H. Bahrami, Z. Z. Haghighi, M. Zahedi, 'Quantum chemical investigation of intramolecular thione-thiol tautomerism of 1, 2, 4-triazole-3-thione and its disubstituted derivatives', J. Mol. Model. **2010**, 16, 841–855.

[34] N. Özdemir, 'Quantum chemical investigation of the intra-and intermolecular proton transfer reactions and hydrogen bonding interactions in 4-amino-5-(2-hydroxyphenyl)-2H-1, 2, 4-triazole-3 (4H)-thione', J. Mol. Model. **2013**, 19, 397–406.

[35] M. Banimustafa, A. Kheirollahi, M. Safavi, S. K. Ardestani, H. Aryapour, A. Foroumadi, S. Emami, 'Synthesis and biological evaluation of 3-(trimethoxyphenyl)-2 (3H)-thiazole thiones as combretastatin analogs', Eur. J. Med. Chem. **2013**, 70, 692–702.

[36] Y. H. Lo, Y. T. Lin, Y. P. Liu, T. H. Duh, P. J. Lu, M. J. Wu, 'Design, synthesis, biological evaluation and molecular modeling studies of 1-aryl-6-(3,4,5-trimethoxyphenyl)-3(Z)-hexen-1,5-diynes as a new class of potent antitumor agents', Eur. J. Med. Chem. **2013**, 62, 526–533.

[37] A. Huczyński, J. Rutkowski, K. Popiel, E. Maj, J. Wietrzyk, J. Stefańska, U. Majcher, F. Bartl, 'Synthesis, antiproliferative and antibacterial evaluation of C-ring modified colchicine analogues', Eur. J. Med. Chem. **2015**, 90, 296–301.

[38] G. M. Morris, R. Huey, W. Lindstrom, M. F. Sanner, R. K. Belew, D. S. Goodsell, A. J. Olson, 'AutoDock4 and AutoDockTools4: Automated docking with selective receptor flexibility', J. Comput. Chem. **2009**, 30, 2785–2791.

[39] R. Huey, G. M. Morris, The Scripps Research Institute Molecular Graphics Laboratory, California, 2008, p. 7–40.

[40] ChemAxon, 2014.

[41] G. M. Morris, D. S. Goodsell, R. S. Halliday, R. Huey, W. E. Hart, R. K. Belew, A. J. Olson, 'Automated docking using a lamarckian genetic algorithm and an empirical binding free energy function', J. Comput. Chem. **1998**, 19, 1639–1662.

[42] M. F. Sanner, 'Python: a programming language for software Integration and development', J. Mol. Graphics. Mod. **1999**, 17, 57–61.

[43] M. Frisch, G. Trucks, H. Schlegel, G. Scuseria, M. Robb, J. Cheeseman, V. Zakrzewski, J. Montgomery Jr, R. E. Stratmann, J. Burant, 'Gaussian 98', Inc., Pittsburgh, PA **1998**.

[44] A. S. Ahmed, E. E. Elgorashi, N. Moodley, L. J. McGaw, V. Naidoo, J. N. Eloff, 'The antimicrobial, antioxidative, anti-inflammatory activity and cytotoxicity of different fractions of four South African Bauhinia species used traditionally to treat diarrhoea', J. Ethnopharmacol. **2012**, 143, 826–839.

[45] Z. Aumeeruddy-Elalfi, A. Gurib-Fakim, F. Mahomoodally, 'Antimicrobial, antibiotic potentiating activity and phytochemical profile of essential oils from exotic and endemic medicinal plants of Mauritius', Ind. Crop. Prod. **2015**, 71, 197–204.